AN ABSTRACT OF THE THESIS OF

RICHARD ALAN HORNING for the MASTER OF SCIENCE
(Name) (Degree)

in CIVIL ENGINEERING presented on October 19, 1971
(Major) (Date)

Title: EXPERIMENTAL BEHAVIOR OF WIDE-FLANGE BEAMS WITH WEB HOLES

Redacted for privacy

Abstract approved: ______________________
T. J. McClellan

Two built-up wide-flange beams with several large holes in each beam were tested to failure. Strains were measured by strain gages at various levels, located at the ends and center of typical holes, and deflections were measured optically at two points on each beam. Lateral bracing was provided to prevent lateral-torsional buckling of the compression flange.

The first beam, with a ratio of hole depth to beam depth of two-thirds, failed by buckling of a web post between adjacent holes. The second beam, with a ratio of hole depth to beam depth of four-fifths, deflected so much that the lateral bracing system failed and the beam failed by lateral buckling of the compression flange. No tearing of the web was observed, due to the rounding of the corners of the holes.

The results of the beam tests correlated well with the Vierendeel theory in the elastic range of stresses, for holes at which there was a

shear force. For holes at which there was no shear, the couple-plus-tee bending theory was somewhat more accurate. Bower's criteria for yielding of the beam section and his lower bound solution for the ultimate strength of the beams were investigated and compared with the loads at which yield actually occurred at each hole. The yield criteria were found to be quite unconservative for these beams, but the predicted ultimate loads for holes with shear forces correlated well with the actual deflections and strains. The points of inflection in the tee sections did not appear to shift significantly from the centerlines of the holes, within the precision of the strain readings.

Deflections were calculated as the sum of the simple beam deflection of the net beam section and deflection of the tee sections as fixed-end beams. The calculated values were 4% to 28% less than the actual deflections in the elastic range.

Experimental Behavior of Wide-Flange Beams with Web Holes

by

Richard Alan Horning

A THESIS

submitted to

Oregon State University

in partial fulfillment of
the requirements for the
degree of

Master of Science

June 1972

APPROVED:

Redacted for privacy

Professor of Civil Engineering

in charge of major

Redacted for privacy

Head of Department of Civil Engineering

Redacted for privacy

Dean of Graduate School

Date thesis is presented October 19, 1971

Typed by Clover Redfern for Richard Alan Horning

ACKNOWLEDGMENT

The writer is indebted to Professors Thomas J. McClellan, John Peterson, and Harold I. Laursen for their advice and assistance in conducting the test program and interpreting the results. Appreciation is also expressed to Fought & Co., Inc., who built and furnished the test specimens, and to Rose' and Breedlove, Inc., who also assisted in the series of projects of which this is a part. The writer also wishes to thank Mr. Edwin Bryan and Mr. John Kellogg for lending tools and assistance in constructing the lateral bracing system and preparing the beams for instrumentation.

Last but not least, thanks to the writer's wife for accepting the role of "thesis widow" without complaint.

TABLE OF CONTENTS

LIST OF FIGURES

Figure		Page
18.	Beam "E," gages L-37, 51. Load vs. strain.	23
19.	Beam "F," gage L-3. Load vs. strain.	24
20.	Beam "F," gage L-6. Load vs. strain.	25
21.	Beam "F," gage L-33. Load vs. strain.	26
22.	Beam "F," gages L-41, 42, 51. Load vs. strain.	27
23.	Beam "E." Location of inflection points.	31
24.	Beam "F." Location of inflection points.	32
25.	Bower's lower bound solution for ultimate strength.	37
26.	Beam "E." Load vs. deflection.	40
27.	Beam "F." Load vs. deflection.	41

LIST OF TABLES

EXPERIMENTAL BEHAVIOR OF WIDE-FLANGE BEAMS WITH WEB HOLES

I. INTRODUCTION

It is obvious that a hole cut through the middle of a steel beam will affect its strength, even if only insignificantly. Several people have conducted research into this problem, to determine quantitatively the size and configuration of hole required to produce an appreciable effect and to measure the magnitude of this effect.

The problem arises when mechanical piping and electrical conduits must be routed through the beams of a building frame. The alternative, to suspend piping under the beams, increases the wasted space between the ceiling of one story and the floor of the next. Thus the owner must buy more building for the same usable space. In order to reduce this dead space and, secondarily, to reduce the dead weight of the steel beams, engineers have resorted to designing the beams with holes sufficiently large to accommodate all piping and conduits. Because of the scarcity of knowledge of the effect of these holes, they are often reinforced with stiffener plates at increased expense. With the increasing use of air conditioning systems the holes must be made larger than previously. The Standard Plaza Building in Portland, Oregon is an example of a building designed with large holes in the beams for mechanical conduits.

The purpose of this study is to enlarge the body of knowledge of this subject by testing actual specimens and comparing measured strains and deflections with computed values. In particular, this study should help verify or disprove the Vierendeel theory (discussed below) and provide some information about the inelastic behavior of beams with holes.

The present study is a continuation of research performed by Cato, Landers and Russell (7, 9, and 12) under the direction of Professor T. J. McClellan. All test specimens were of the same cross section and, except for Cato's, of the same length, differing only in the size of holes. Two beams were tested in this study. Strains were measured at various points by electrical resistance type gages, up to the limit of the reading equipment or the gage adhesive, and deflections were measured optically at two points. The beams were loaded well into the inelastic range and local inelastic strains were measured before a buckling failure occurred.

II. REVIEW OF THEORY

Several different methods of predicting the stresses in a beam with web holes have been advanced. Perhaps one of the simplest idealizes the action in the vicinity of the hole as that of a couple acting through the centroidal axes of the upper and lower tees, plus the tees themselves acting as fixed-end beams under a shear type loading (8, p. 34). (See Figure 1a.). The Vierendeel theory assumes that the stresses on any cross-section are equal to the algebraic sum of the flexural stress in the beam as a whole, based on the net section (i.e., excluding the hole), and the flexural stress on the tee sections as cantilever beams caused by the shear at the center of the hole (11, p. 160; 12, p. 24). (See Figure 1b.) Opinion varies as to the division of the shear between upper and lower tees, whether it be based on the areas, flexural stiffnesses, or shear stiffnesses of the tee sections (2, p. 803); however, for tees of identical cross-section the results are the same, as is the case in this study. Russell discovered that the Vierendeel theory becomes more accurate if the point of inflection in the tees is not assumed to be above and below the center of the hole, as is the customary practice. For his beams, which were built and loaded similarly to those the writer tested, Russell discovered that the point of inflection shifts from the centerline of the hole toward the end where the bending moment is lesser (12, p. 27).

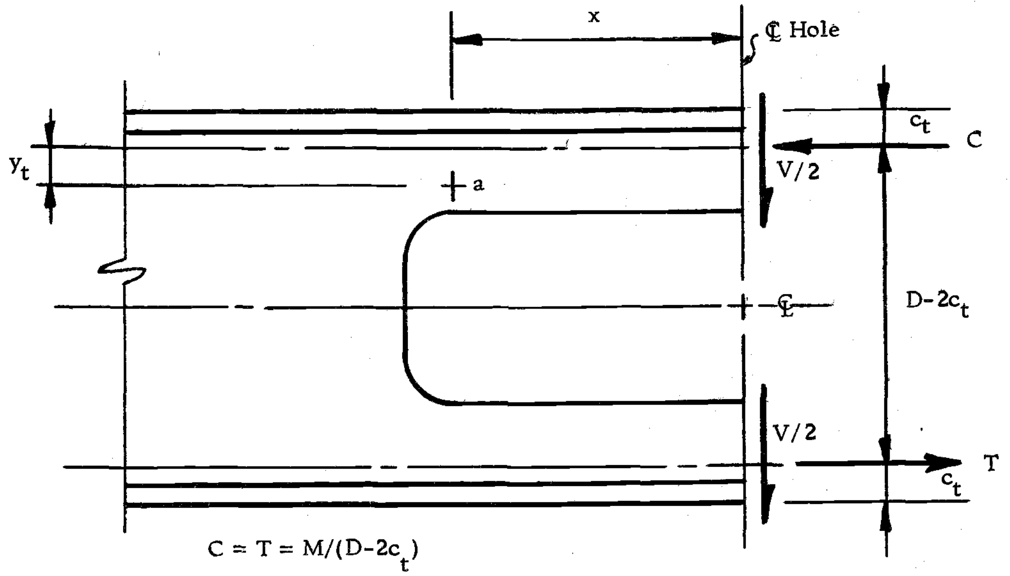

$C = T = M/(D-2c_t)$

$f_t = C/A_t + Vxy_t/2I_t$ at point "a"

a) Couple plus tee-bending theory

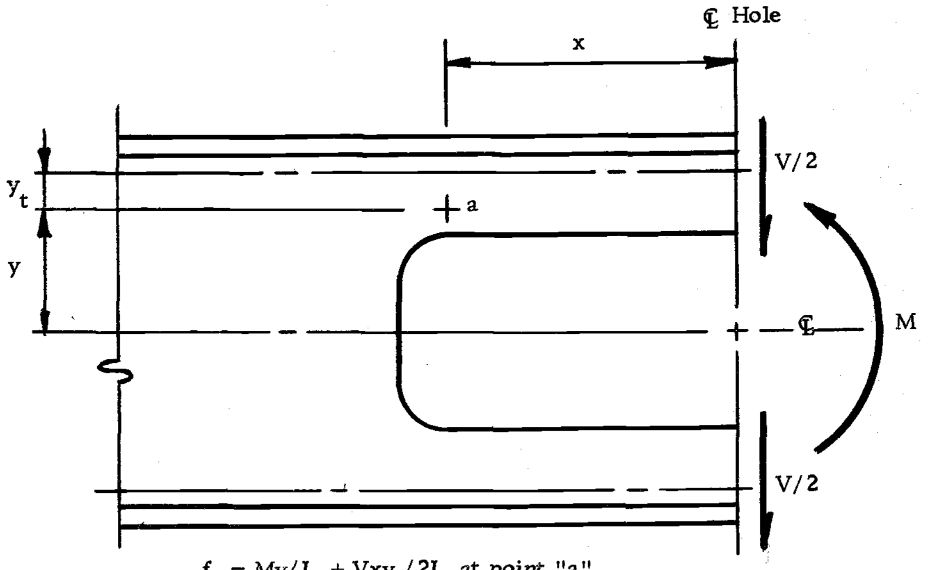

$f_b = My/I_b + Vxy_t/2I_t$ at point "a"

b) Vierendeel theory

Figure 1. Theories of structural action.

Neither theory described above accounts for the stress concentrations present at the corners of the holes. Bower has reported a method based on the theory of elasticity which gives reasonably accurate predictions of the octahedral shear stresses at the corners of the holes (3, 4). The significance of octahedral shear stresses is that they give the best combination of simplicity of analysis and accuracy of prediction of yielding for ductile metals such as structural steel. One disadvantage of the method is that it appears to be quite complicated and dependent upon a computer analysis. There is also the question of whether these stress concentrations at the corners of the holes are the controlling factor in failure of beams with web holes.

Although the subject of stress analysis has received much attention, there does not appear to be any guideline as to what limits should be placed on these stresses, whether the nominal flexural stresses in the tee sections or the stress concentrations at the corners of the holes. The writer infers that the nominal flexural stresses calculated by Vierendeel theory or other method should be limited to the allowable flexural stress in a beam without web holes, and that the stress concentrations at the corners should be limited to the yielding shear stress divided by an appropriate factor of safety.

Bower (2, p. 793) has proposed a design procedure based upon an interaction diagram for flexural and shear stresses calculated on the gross cross section of the beam, but modified according to the geometry of the hole and certain properties of the beam cross-section. The boundaries of the interaction diagram are the ratios of the allowable stresses for beams with web holes to the allowable stresses for beams without holes, giving the design engineer a convenient method of checking the adequacy of a beam. Bower states that the method as it applies to rectangular holes is based on the Vierendeel analysis but makes no attempt to include the effect of stress concentrations at the corners of the holes, because these are of such a large magnitude that design against yielding is impractical.

The writer has found little information on deflections of beams with web holes, whether methods of calculation or experimental results. Russell discovered that the effect of the holes is a significant increase in deflection from that which would be predicted for beams without holes (12, p. 15). By including the beam action of the tees above and below the holes, Russell was able to better predict the deflections of his beams, especially when the actual width of the web post between adjacent holes was taken into account.

III. APPARATUS AND PROCEDURES

Two test specimens were fabricated from A-36 steel plate, welded to form 15-inch by 4-inch I-beams 12 feet long. Five holes were cut in the web of each beam after fabrication, symmetrically placed about the centerlines of the beams. The corners of each hole were cut smoothly to a one-inch radius. The remaining length of web plate between each hole was six inches; the length of web at the ends of the beams was also six inches. The beam dimensions and configuration of the holes are shown in Figure 2. The basic cross-section is the same as in previous research by Cato, Landers and Russell, and except for the length and height of the holes, the test beams are identical with Russell's beams. After completion of the testing program, one-half inch square coupons were cut from the flanges of the beams and their yield stress in tension determined. The value determined experimentally was approximately 36 kips per square inch (ksi).

The test beams were loaded in a Riehle screw-type testing machine of 150-kip capacity, using a system of beams and rollers to distribute the load equally into four parts, as indicated in Figures 2 and 5. Two small A-frames built up from angles were fastened to the floor beside the testing machine with concrete anchors to provide lateral bracing. Additional bracing was provided at the center of the beam by angles and flat bars wedged into openings in the testing

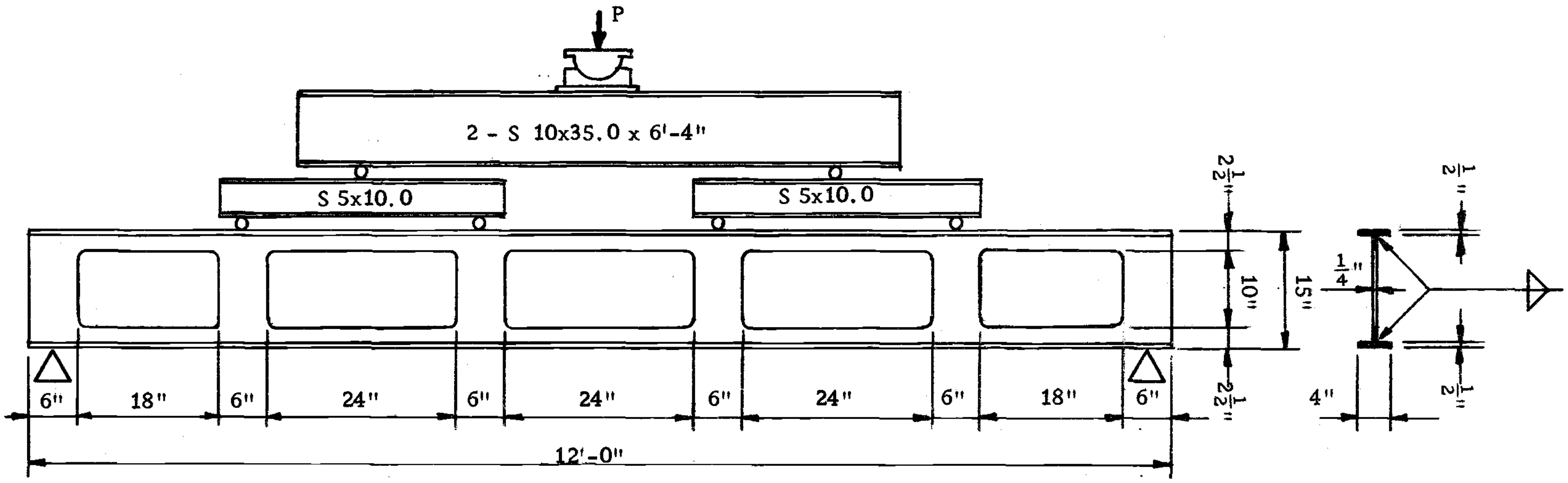

a) Beam "E" and loading system

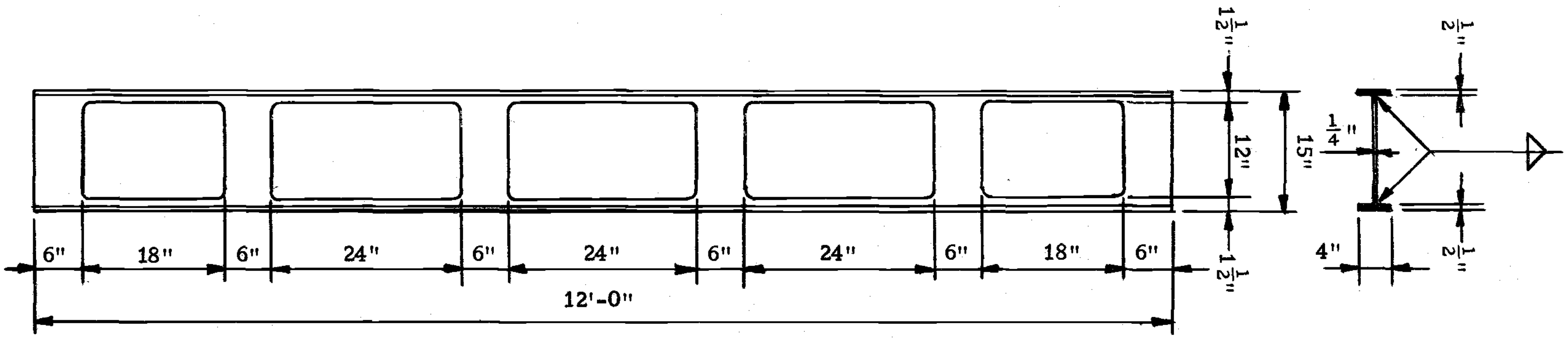

b) Beam "F"

Figure 2. Test specimen dimensions and loading system.

machine column. U-shaped clips were then fastened to the upper flange of the beam and connected to the A-frames and the testing machine column. The bracing scheme is illustrated in Figure 3. Strains were measured by Baldwin-Lima-Hamilton electrical resistance strain gages type SR-4, cemented to the beams in the locations indicated in Figure 4. A BLH strain gage converter and several switching units gave a digital readout of strains to a potential precision of ± 25 microinches per inch. Strips of graph paper were cemented to the web plates between holes at the horizontal centerlines of the beams, and a thin wire stretched from end to end of the beams at their centerlines. By sighting through small telescopes on fixed stands, the deflections of the beams were optically measured as the movement of the graph lines relative to the wire, which was assumed not to move. The arrangement of test equipment is shown in Figures 5 and 6.

For each beam, increments of load were applied up to the anticipated yield point of the most highly stressed part of the beam, then released and the strains at zero load read. Several such cycles were conducted for each beam to determine its behavior in the elastic range. Then increments of load were applied and the beams tested to failure, although in each case the loading had to be halted during the series due to time limitations. Beam "E," with the smaller holes, was loaded in increments of 2 kips at a rate of 0.103 inches per

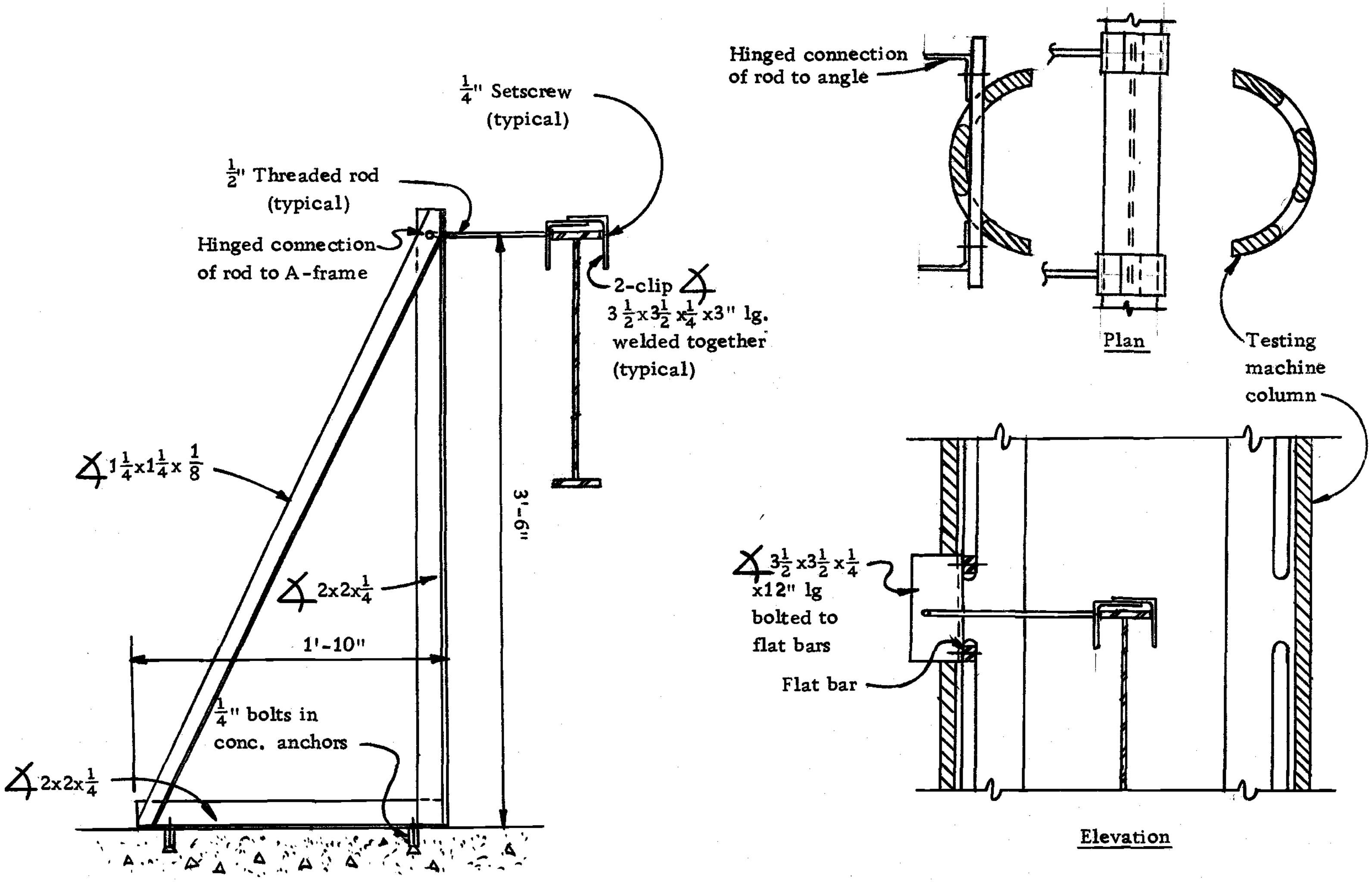

a) Detail @ ends of beam

b) Detail @ center of beam

Figure 3. Lateral bracing details.

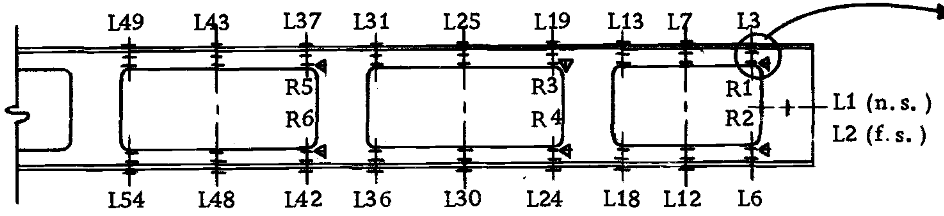

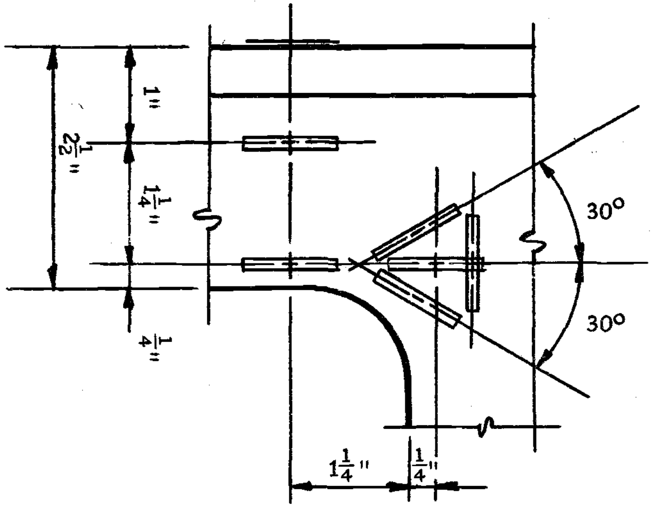

a) Beam "E"

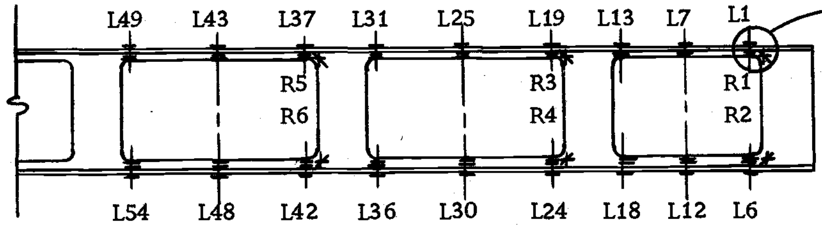

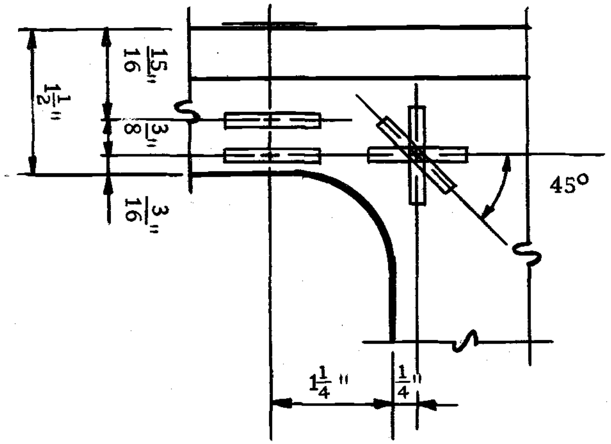

Note: Gage L4-A f.s. of L4
Gage L15-A f.s. of L15

b) Beam "F"

Figure 4. Strain gage locations.

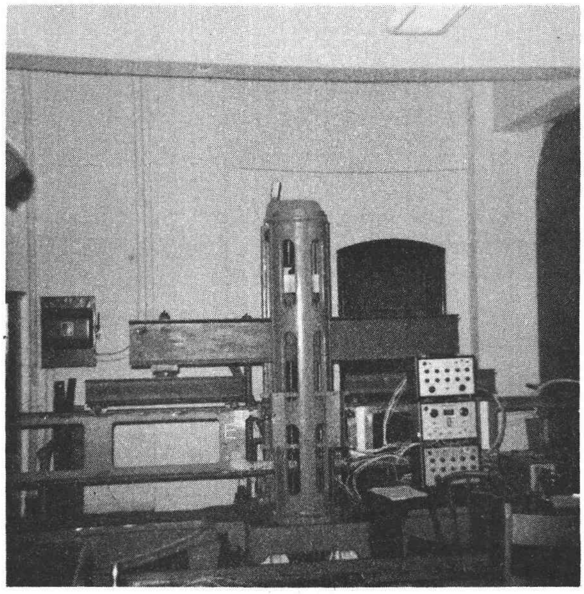

Figure 5. Typical method of applying load and arrangement of equipment.

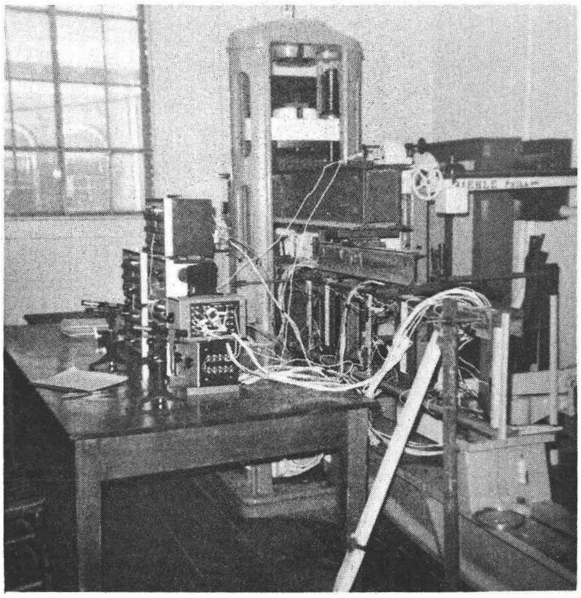

Figure 6. Typical arrangement of equipment.

minute motion of the loading head up to a total of 8 kips of load; in the final series, it was loaded in the same increments at a rate of 0.056 inches per minute to a total of 22 kips, the load released for three days, the beam loaded to 24 kips, the load released for three hours, and the beam finally loaded to failure. Beam "F" was loaded in increments of 1 kip at a rate of 0.103 inches/min. to 3 kips for several cycles, then at a rate of 0.056 inches/min. to total loads of 6, 7 and 8 kips, the load was released for three days, and finally the beam was loaded to failure. A typical cycle of applying an increment of load and reading the strains and deflections required approximately half an hour. The order of steps was: apply the load, read and record strains going from the end of the beam to the center, and read and record deflections. No attempt was made to maintain the load constant during the readings, even though deflection of the beam during the 25 minutes or so required to read strains resulted in gradual reduction of the load in the inelastic range.

IV. RESULTS AND DISCUSSION

A. General Observations

Beam "E" began to show noticeable deflection at a total load of about 22 kips. As deflection progressed, the rate of loading in kips per minute decreased either due to formation of plastic hinges or buckling of the web posts between adjacent holes. At a total load of 29.1 kips, deflection occurred at the same rate as application of load or faster, and the load on the beam gradually decreased. At somewhat less than the maximum load, the writer noticed severe buckling of the first interior web post on the non-instrumented end of the beam. There was slight local buckling at one corner of the end hole at the instrumented end of the beam. (See Figures 7-10.)

Beam "F" began to show noticeable deflection at a total load of about 11 kips. Deflections were considerably greater than for Beam "E," and rendered the lateral bracing system ineffective. At two or three levels of loading the load remained constant or dropped momentarily, then increased again as the rate of deflection diminished. When the beam "bottomed out" on the bed of the testing machine (a deflection of 8-1/2 inches!), the writer inspected it and discovered severe lateral buckling of the upper flange. However, the beam had been accepting an increasing load at the same rate of loading head motion and carried a total of 17.3 kips just before it ran out of room

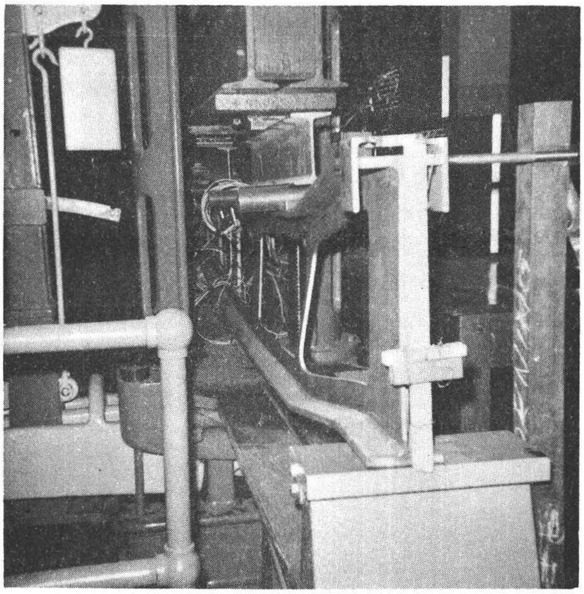

Figure 7. Beam "E." Buckling of first interior web post. Total load = 24.5 kips.

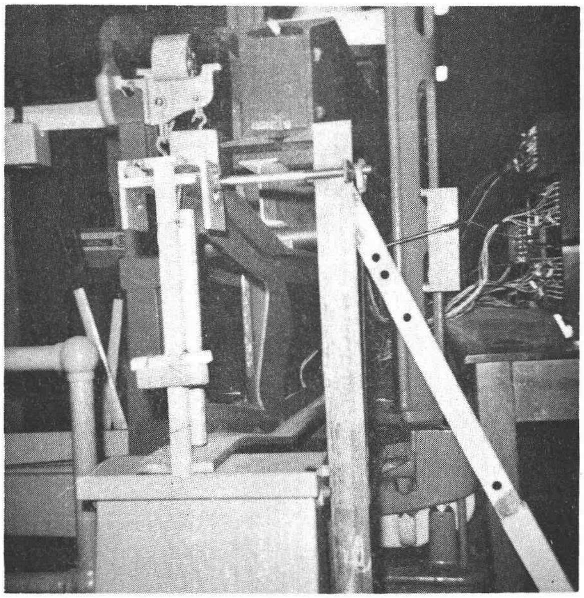

Figure 8. Beam "E." Buckling of interior web post. Total load = 24.5 kips.

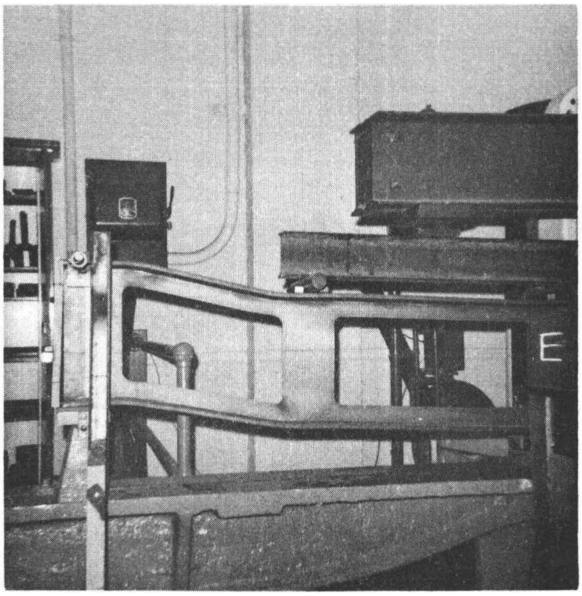

Figure 9. Beam "E," total load = 24.5 kips. Plastic hinges at corners of end hole.

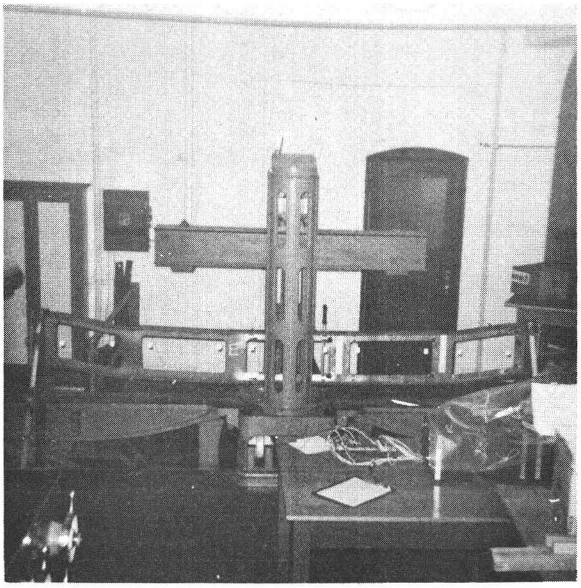

Figure 10. Beam "E." Residual deflections after load was completely released. (Paper strips inside web holes indicate original location of beam centerline.)

to deflect. (See Figures 11-14.) The strains at the corners of the end hole were apparently large enough to cause failure of the strain gage adhesive in two places, making it necessary to cement new gages on the opposite side of the web. Despite the severe distortion of the tee sections in both beams, no tearing of the webs was observed and only a small degree of buckling at one corner was apparent.

B. Comparison of Theoretical and Measured Strains

As noted in Figure 1, the Vierendeel theory predicts the stresses in the tee section as

$$f_b = \frac{My}{I_b} + \frac{Vxy_t}{2I_t} \qquad (1)$$

where I_b and I_t are the moments of inertia of the net beam section and the tee section respectively, and x, y and y_t are distances to the point in question from the point of inflection in the tee and from the centroidal axes of the beam and the tee, with signs determined by the direction to the point in question. The longitudinal strain is given by

$$\epsilon = \frac{f_b}{E}$$

Figures 15 through 22 show typical examples of the variation of the measured strains with the applied load and the relation predicted by

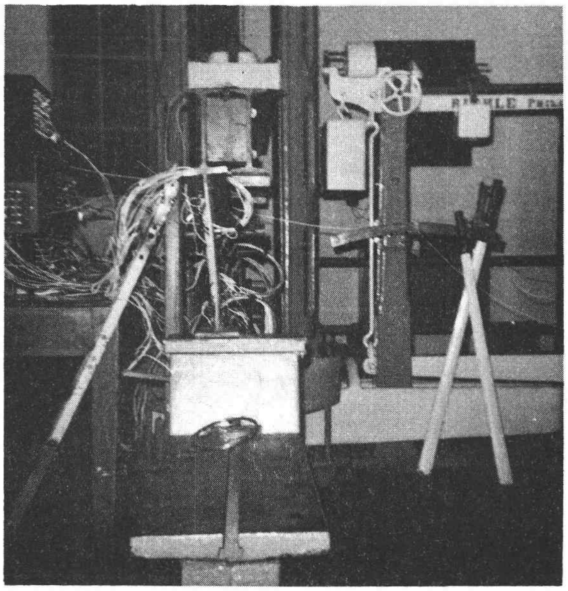

Figure 11. Beam "F," total load = 17.3 kips. Lateral buckling of compression flange.

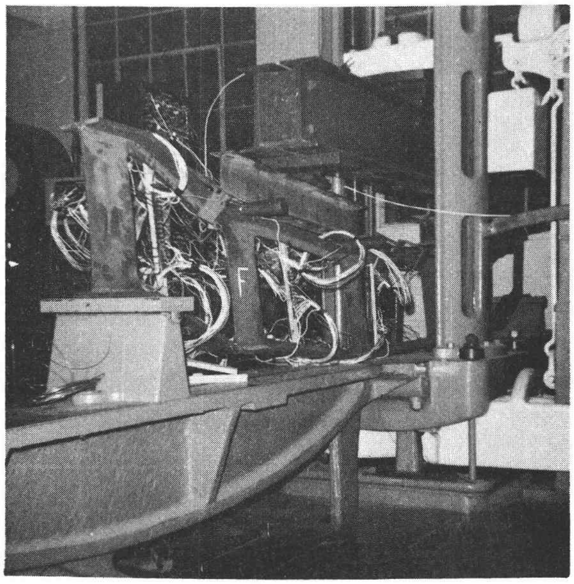

Figure 12. Beam "F," total load = 17.3 kips. Extreme deflection of beam has rendered lateral bracing at near end and center of beam ineffective, resulting in lateral buckling.

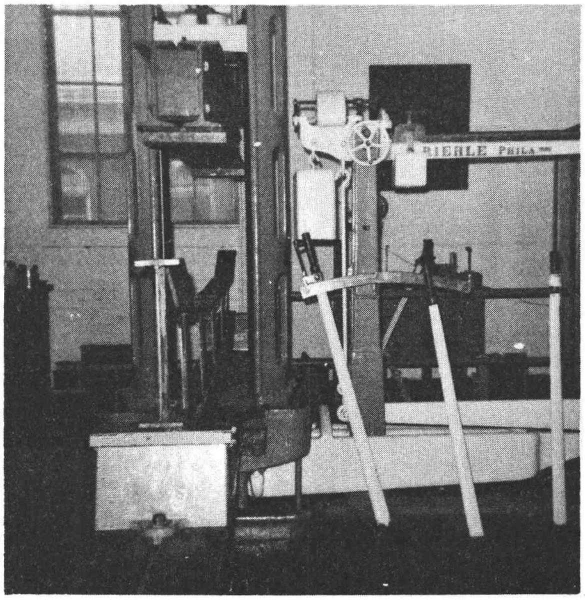

Figure 13. Beam "F." Residual deflection.

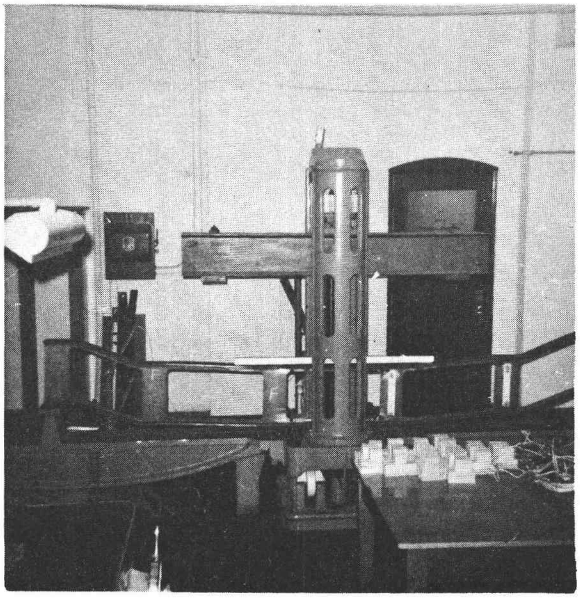

Figure 14. Beam "F." Residual deflection.

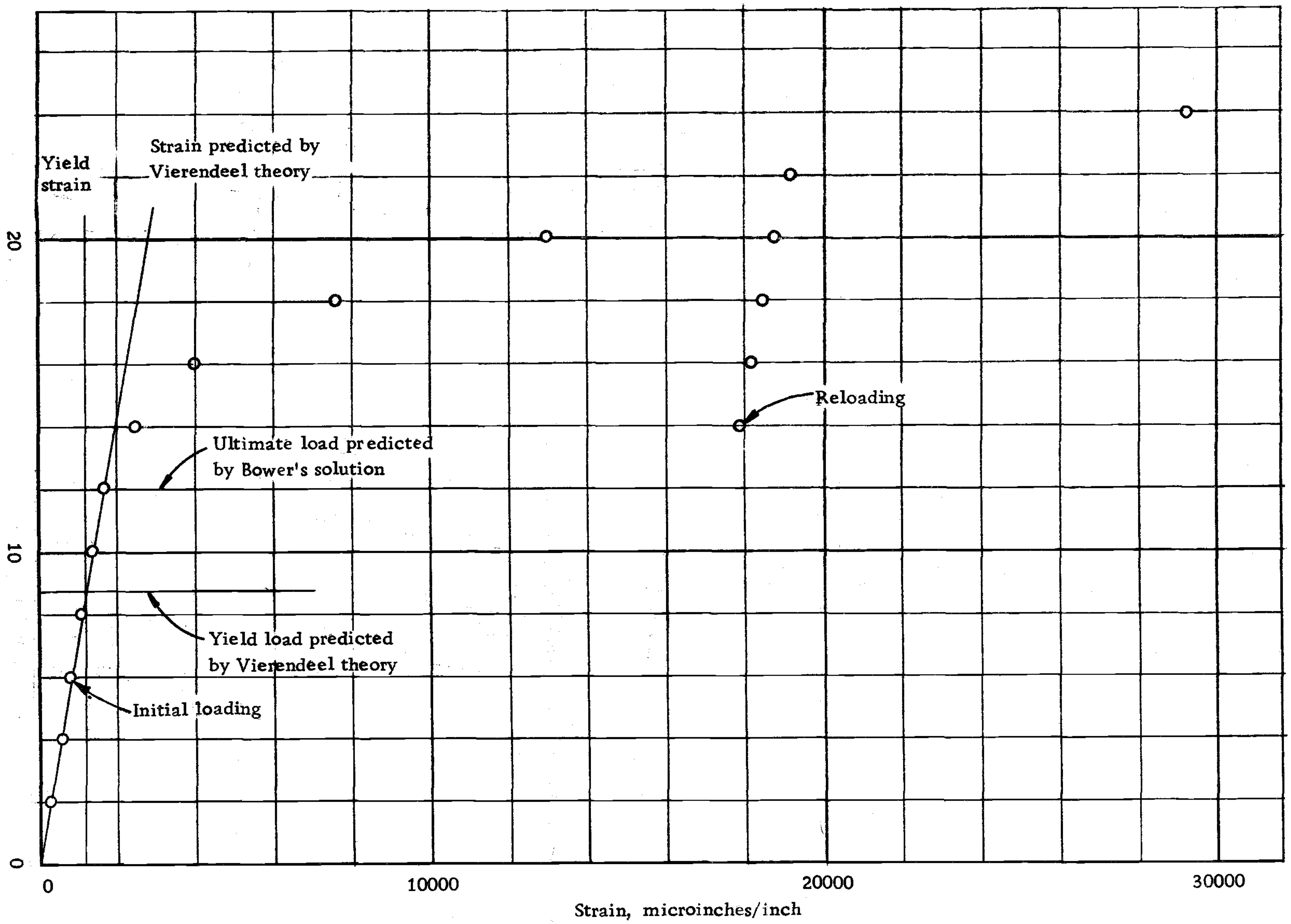

Figure 15. Beam "E," gage L-4, load vs. strain.

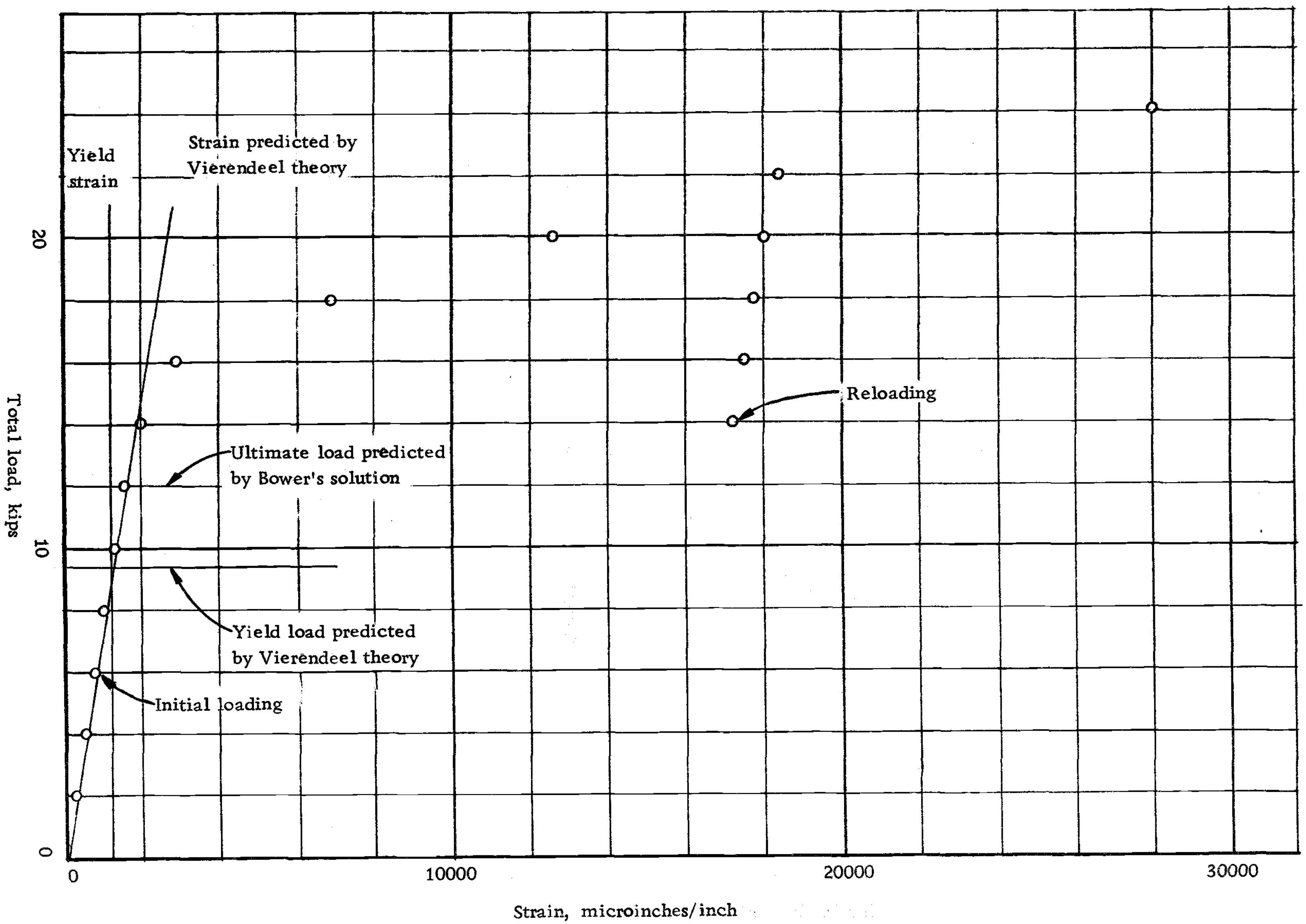

Figure 16. Beam "E," gage L-16, load vs. strain.

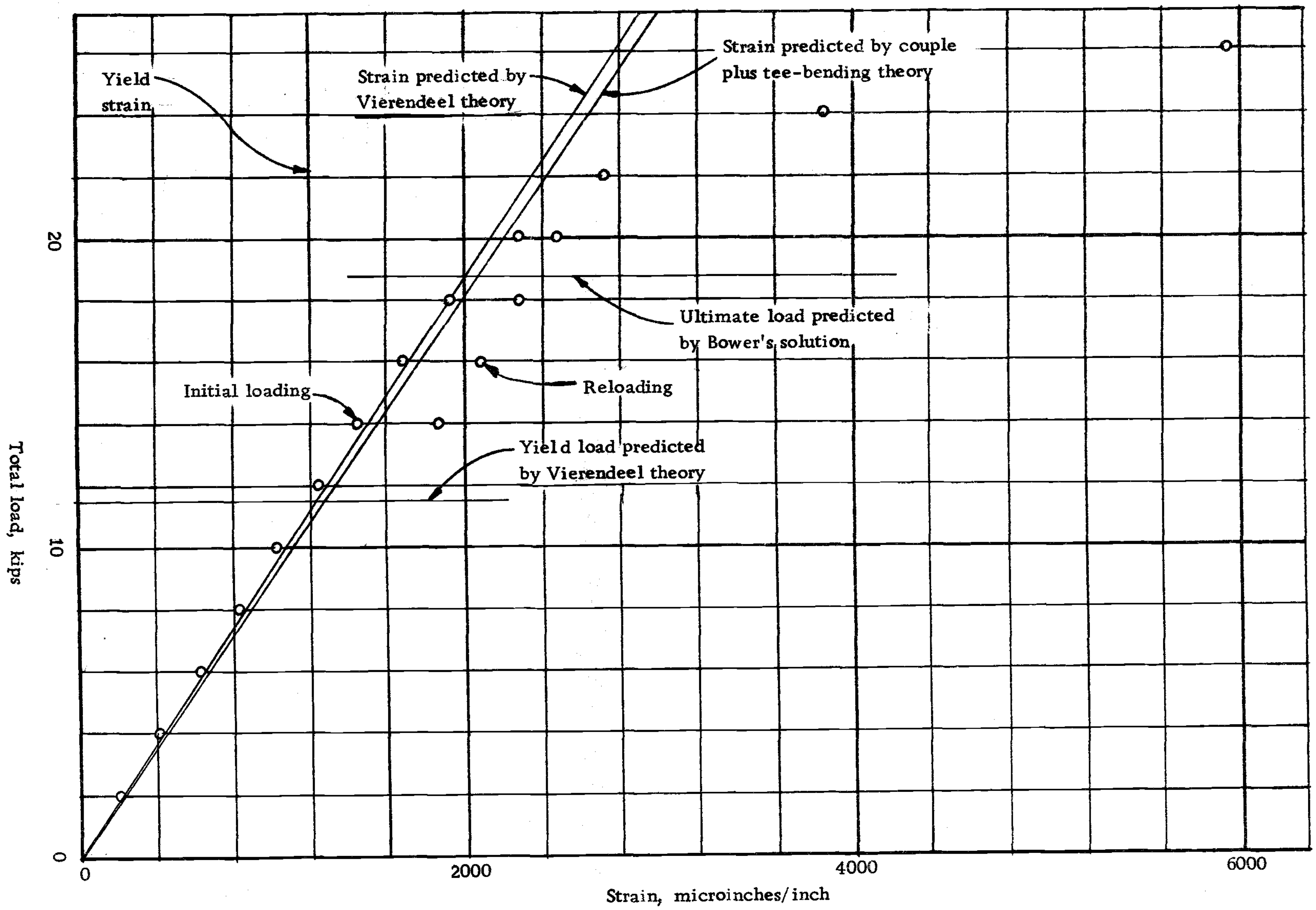

Figure 17. Beam "E," gage L-21, load vs. strain.

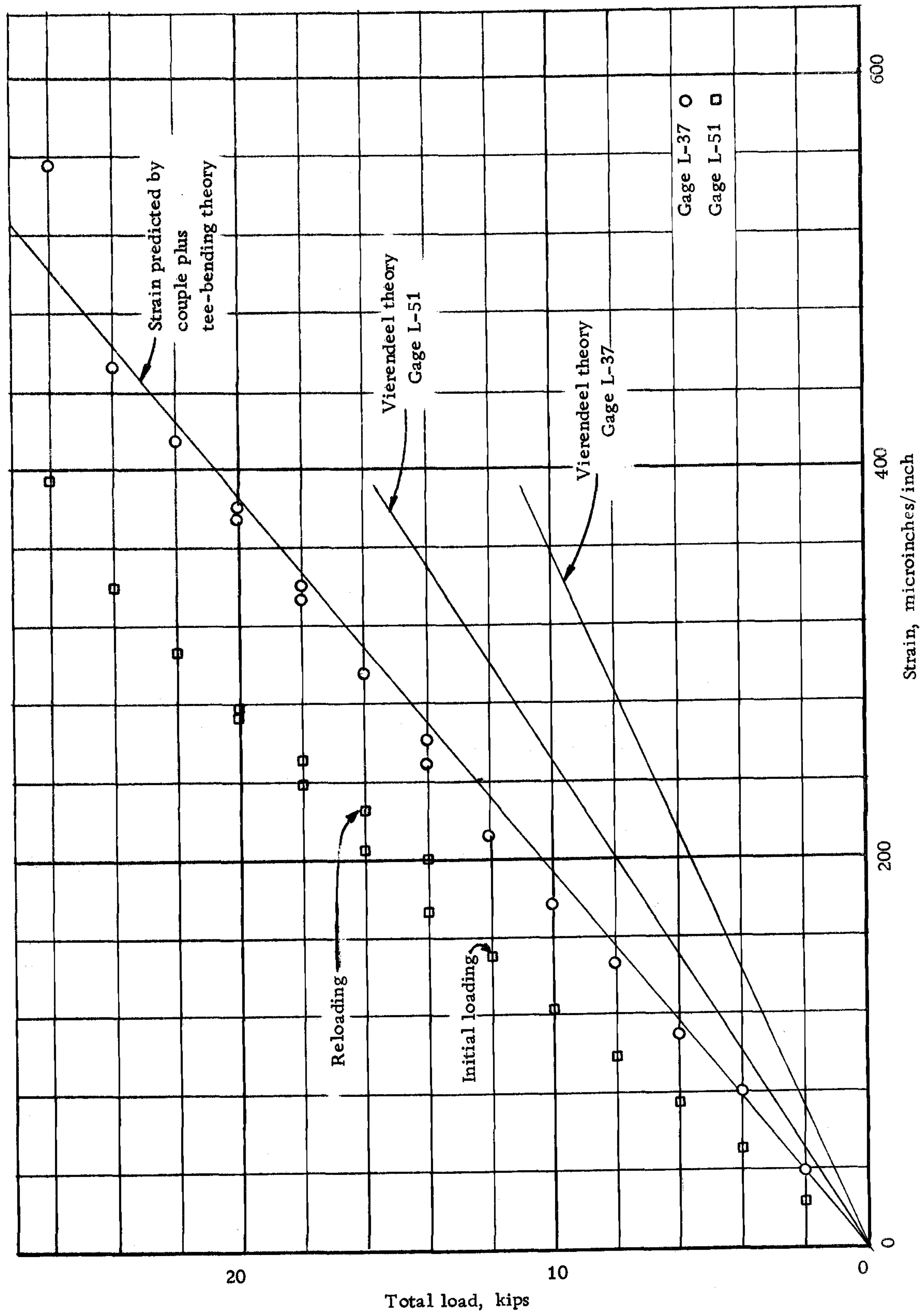

Figure 18. Beam "E," gages L-37, 51. Load vs. strain.

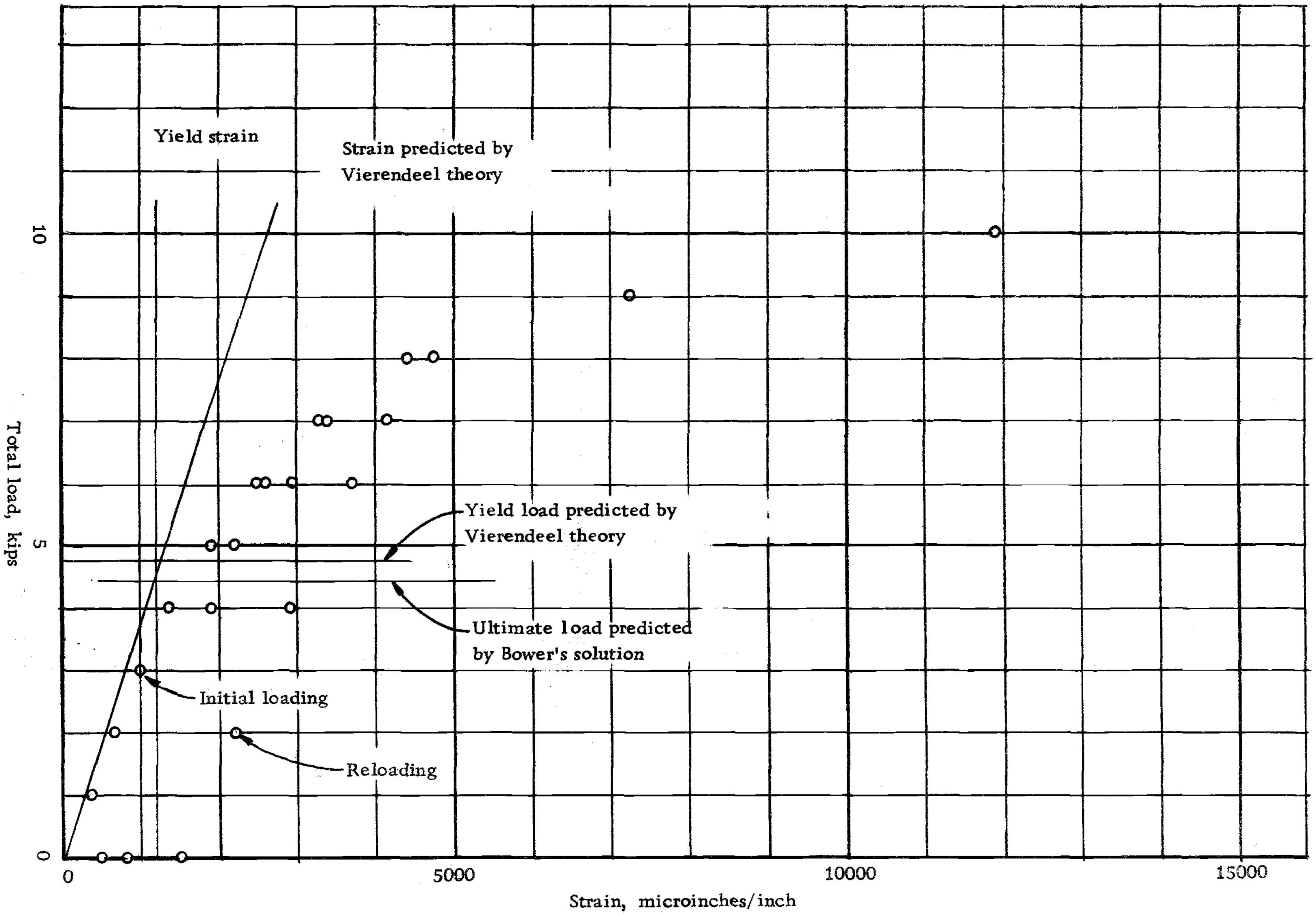

Figure 19. Beam "F," gage L-3. Load vs. strain.

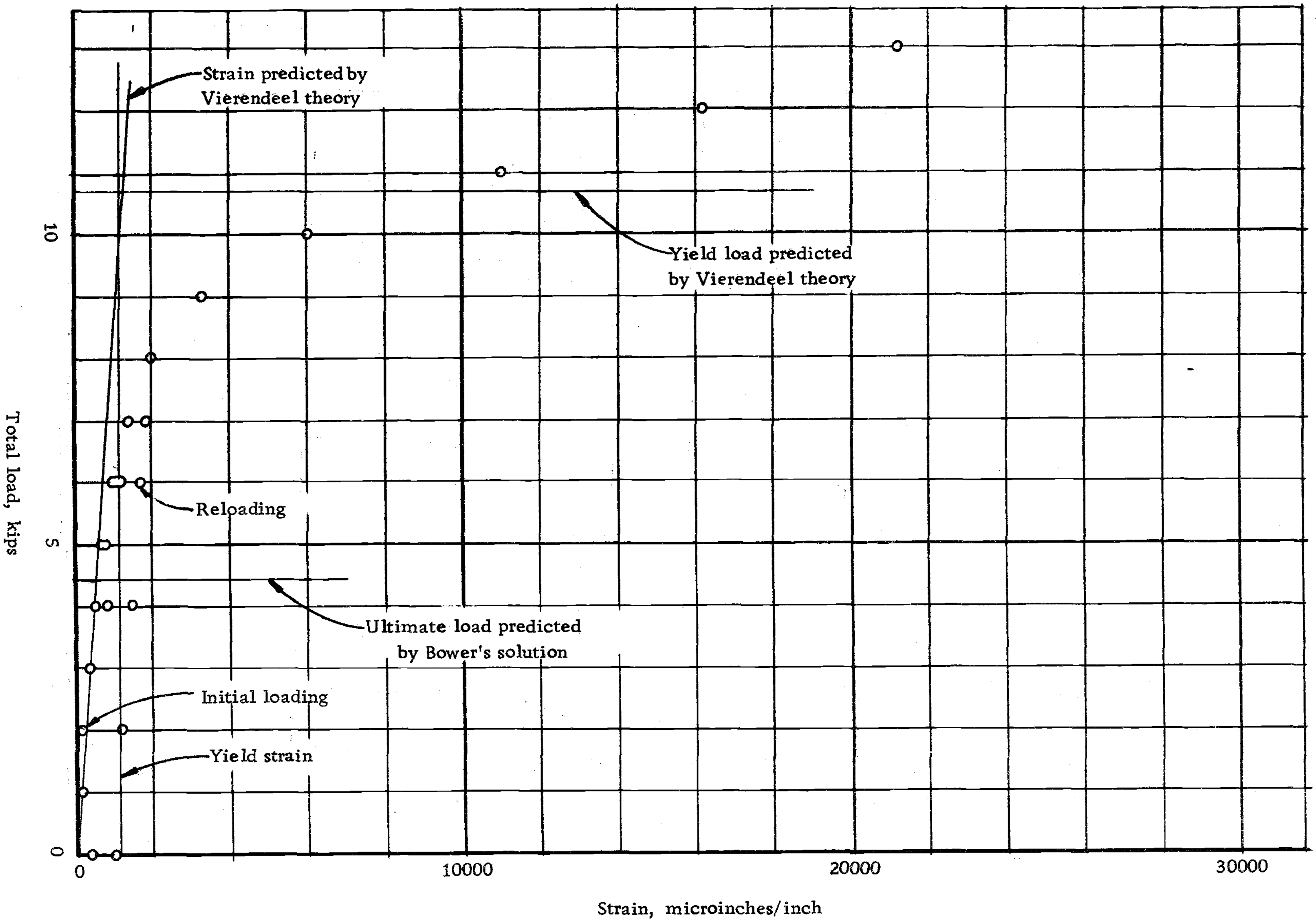

Figure 20. Beam "F," gage L-6. Load vs. strain.

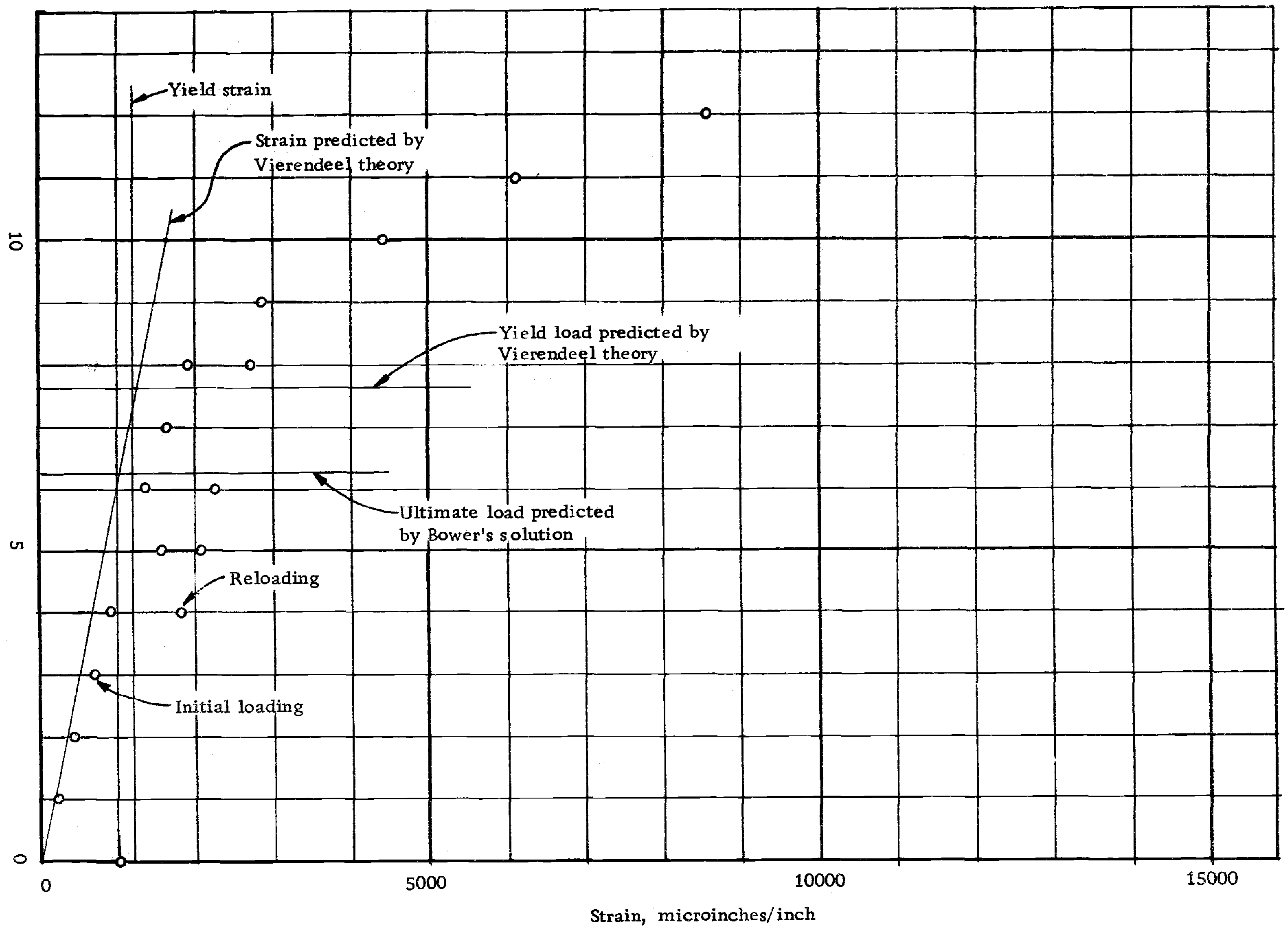

Figure 21. Beam "F," gage L-33. Load vs. strain.

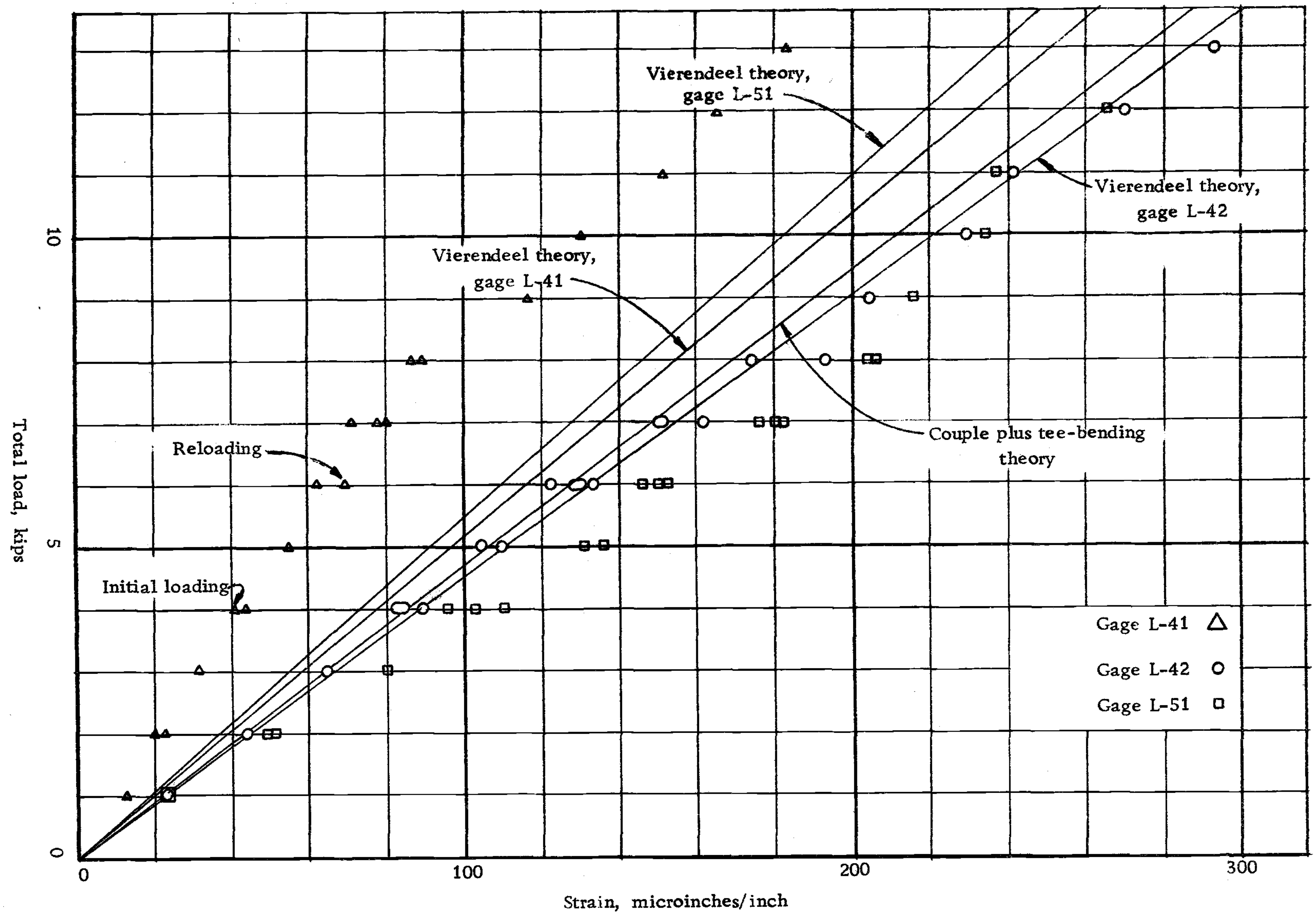

Figure 22. Beam "F," gages L-41, 42, 51. Load vs. strain.

the Vierendeel theory for elastic stresses. As indicated, the correlation of actual and theoretical strains was good for the two holes in each beam for which $V \neq 0$. For the center hole in each beam, at which there was no shear, the predicted strains were consistently greater than the actual strains in Beam "E" (see Figure 18); for Beam "F," there was no such consistency, with theoretical strains being greater than actual at some gages, lesser at other gages, and in good agreement at the remainder. The pattern of variation also differed from one side of the hole to the other. (See Figure 22 for typical examples.) Also indicated on the charts is the strain at which yielding should begin at each gage (indicated as 1200 microinches per inch; more accurately, $\epsilon_y = F_y/E = 36$ ksi/29000 ksi = 1240 microinches per inch). Note that for many gages, yielding did not begin until strains had considerably exceeded this level.

An alternate theory visualizes the beam as a Vierendeel truss, for which (see Figure 1)

$$f_t = f_a + f_b = \frac{M}{A_t(D-2c_t)} + \frac{Vxy_t}{2I_t} \qquad (2)$$

in which A_t is the area of one tee and $(D-2c_t)$ is the distance between the centroidal axes of the upper and lower tee sections. Note that the second term of the expression is identical with that for the Vierendeel theory. In fact, for Beams "E" and "F" this term accounted for most of the strain at the gages where a shear force existed. In Figures 15, 16, 19, 20 and 21 the Vierendeel theory and "couple plus tee-bending theory" gave the same results at the scale of the chart. For the center holes of the beams, where $V = 0$ and the second term of the stress equation vanishes, the latter equation appeared to be in better agreement with measured strains than the Vierendeel theory, with a few exceptions. In general, the "couple plus tee-bending theory" was either in good agreement with the actual strains or less conservative than the Vierendeel theory (see Figures 18 and 22).

Table 1. Beam properties for elastic analysis.

Beam	D in.	I_G in.^{4}	I_B in.^{4}	A_t in.^{2}	C_t in.	I_t in.^{4}	Hole	$\frac{V}{P}$	M/V in.
							End	.50	4.76-20.24
E	15	267.50	246.67	35.00	.50	.8333		.25	53.24-74.8
							Ctr.	0	∞
							End	.50	4.76-20.24
F	15	267.50	231.50	32.26	.33	.1875		.25	53.24-74.8
							Ctr.	0	∞

A basic assumption in the presentation above is that the point of inflection in the tee sections from which the dimension "x" is measured is at the centerline of the hole. In order to determine the actual location of the point of inflection, strain gages were applied in three rows and three columns to the tees above and below three holes in each beam. The most significant part of the stress equation is the term $Vxy_t/2I_t$; at the point of inflection $x = 0$ and this term vanishes. Also, for gages at the same level but on opposite sides of and equal distances from the point of inflection, the values of this term must be equal and opposite. If the strains for all the gages on a tee are plotted at the horizontal location of the gages, the results should be three straight lines connecting the strains at each level of the tee; furthermore, these lines should intersect in a common point, at the location of the inflection point. (The term $M/(A_t(D-2c_t))$ is a constant for any point in the tee; the term My/I_b varies slightly, but makes up only a fraction of the total stress, therefore its variation should be negligible.) Figures 23 and 24 show these strains plotted for Beams "E" and "F" respectively, for the holes where $V \neq 0$. A slight shift of the inflection point from the centerline of the hole can be observed for some of the tees, but the effect appears to be insignificant, and unwarranted for a hand computation. For the holes for which $V = 0$, there should be no point of inflection in the tees and the stresses should be uniform along the tees at any given level. This was observed for the center hole in Beam "E," within the precision of the gage readings; the measured strains were not uniform at the center hole in Beam "F," but because of the low magnitudes of the strains the significance of this observation is doubtful. The strain differences at the maximum load were only twice the possible error in the gage

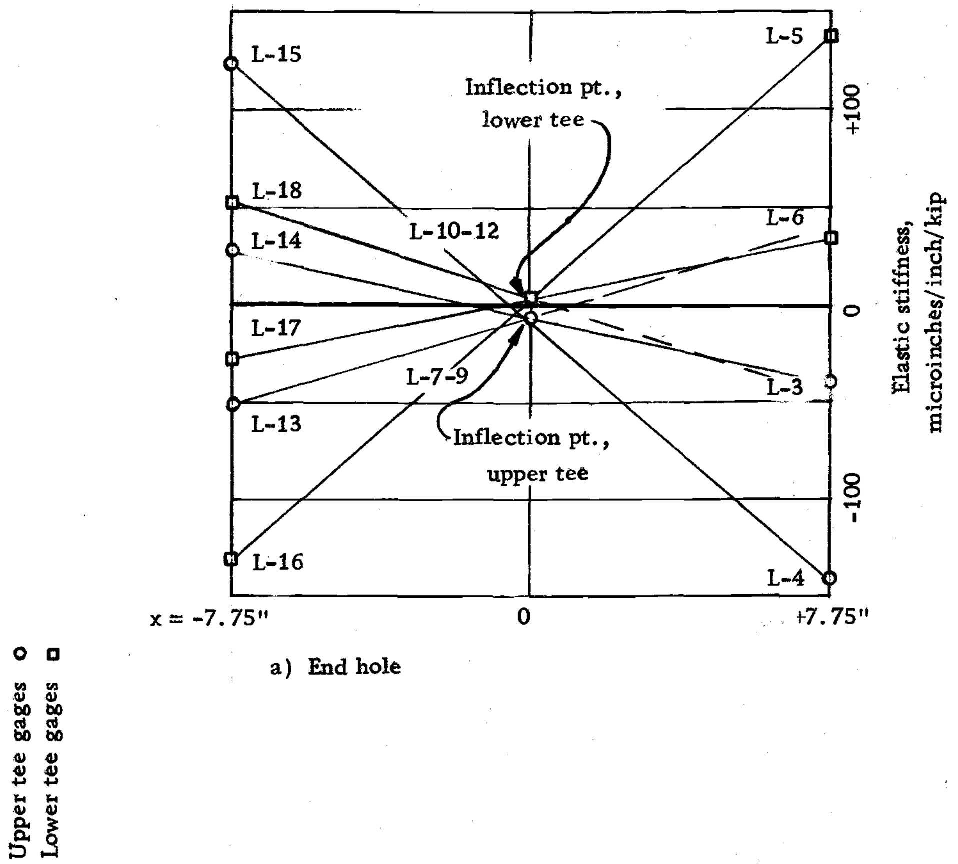

a) End hole

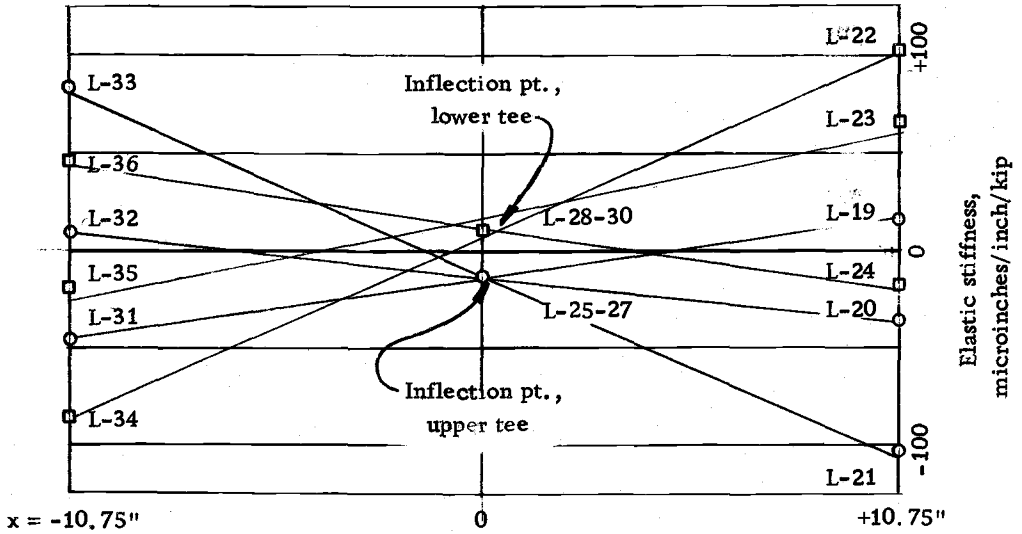

b) First interior hole

Figure 23. Beam "E." Location of inflection points.

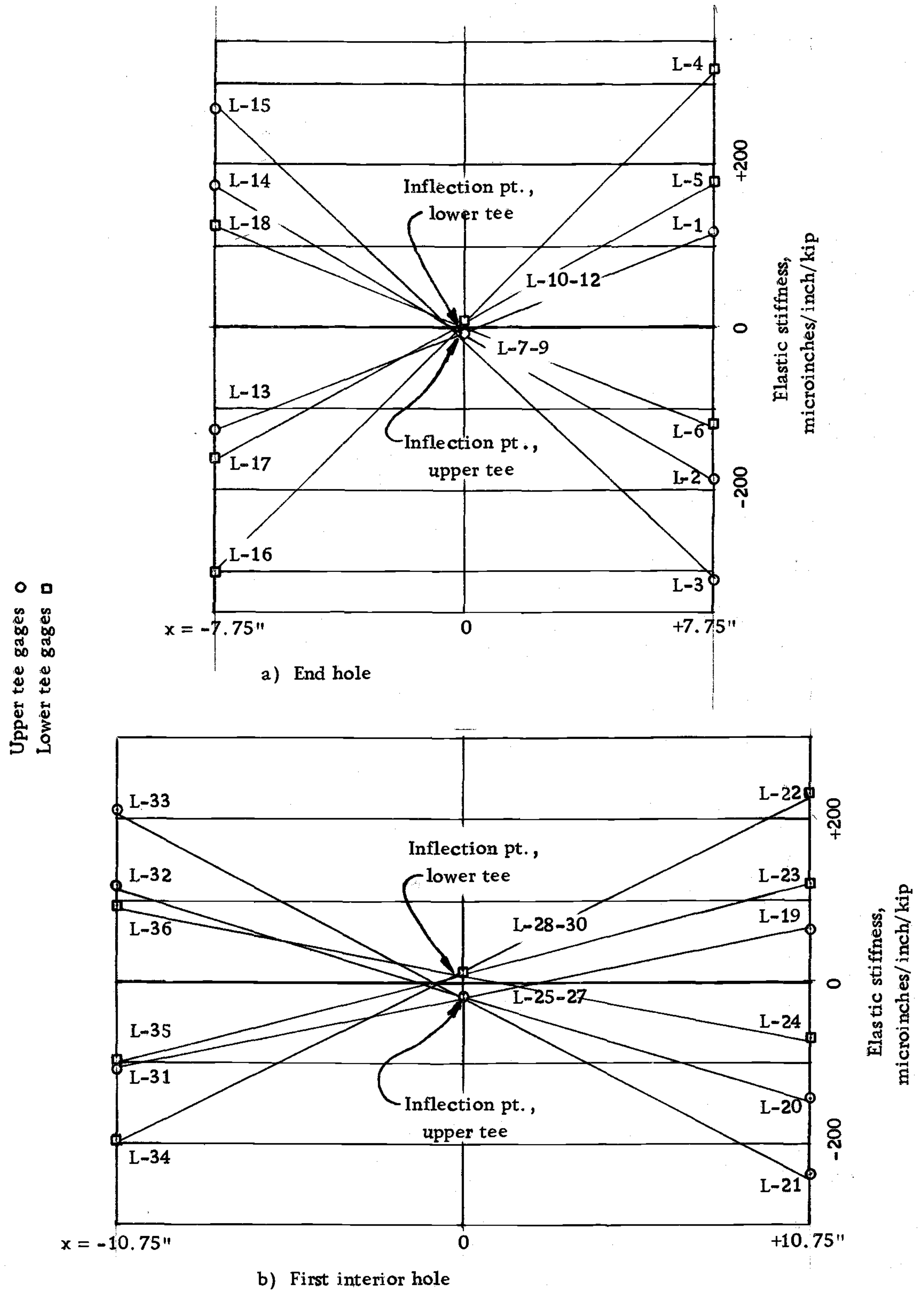

Figure 24. Beam "F." Location of inflection points.

readings (± 25 microinches per inch).

Rosette gages were applied to the web at the upper and lower corners of the low-moment edge of each hole. The principal strains recorded were in most cases less than the measured strains for the adjacent linear gages. Research has shown that significant stress concentrations exist at the corners of the holes (see Refs. 3 and 4), but they were apparently undetected by the rosettes. Because the data available from these gages do not appear to provide any significant information, none of the data has been presented here.

C. Prediction of Yield Load

Because of the good agreement between the Vierendeel theory and measured strains, it would be reasonable to expect the yield load for the beams to be the load at which the Vierendeel stresses reach the yield stress of the grade of steel being used. This load is indicated in Figures 15 through 22, 26 and 27. For Beam "E," the measured strains and deflections indicate yielding at a load of approximately 12 kips, compared to 8.73 kips predicted by theory. For Beam "F" the agreement is better, with the yield load being about 4 kips compared to 4.74 kips predicted.

Bower (2, p. 784) has published equations for yielding of beams with rectangular web holes based on the von Mises and Vierendeel theories. On the low-moment side of the hole, at the edge of the hole, the yield criterion is

$$\left(\frac{H}{D}\right)\left(\frac{a}{H}\right)\left[\frac{8\left(1+\frac{4A_f}{A_w}-\frac{H}{D}\right)}{\left(1-\frac{H}{D}\right)^2\left(1+\frac{8A_f}{A_w}-\frac{H}{D}\right)}\right]\frac{f_{vg}}{F_v}+\left(\frac{H}{D}\right)\left[\frac{1+\frac{6A_f}{A_w}}{1+\frac{6A_f}{A_w}-\left(\frac{H}{D}\right)^3}\right]\frac{f_{bg}}{F_b}=\frac{5}{3} \tag{3}$$

where f_{vg} and f_{bg} are the shear and bending stresses computed using the gross beam cross section, a is half the length of the hole, and H is the height of the hole. On the high-moment side of the hole, at the intersection of the web and the flange, the yield criterion is

$$\left[\frac{\frac{4}{3}+\frac{64\left(\frac{H}{D}\right)^2\left(\frac{a}{H}\right)^2}{\left(1+\frac{8A_f}{A_w}-\frac{H}{D}\right)^2}}{\left(1-\frac{H}{D}\right)^2}\right]\left(\frac{f_{vg}}{F_v}\right)^2+\left[\frac{16\left(\frac{H}{D}\right)\left(\frac{a}{H}\right)\left(1+\frac{6A_f}{A_w}\right)}{\left(1-\frac{H}{D}\right)\left(1+\frac{8A_f}{A_w}-\frac{H}{D}\right)\left(1+\frac{6A_f}{A_w}-\left(\frac{H}{D}\right)^3\right)}\right]$$

$$\times\left(\frac{f_{vg}}{F_v}\right)\left(\frac{f_{bg}}{F_b}\right)+\left[\frac{1+\frac{6A_f}{A_w}}{1+\frac{6A_f}{A_w}-\left(\frac{H}{D}\right)^3}\right]^2\left(\frac{f_{bg}}{F_b}\right)^2=\frac{25}{9} \tag{4}$$

By substituting f_{vg} and f_{bg} as functions of the load P into these equations, together with the known properties of the beams (see Table 2), each equation can be solved for the yield load P_y directly.

Bower's equations have been verified for beams with ratios of H/D of 0.6 or less. For beams outside this range (such as the writer tested) Equation 4 appears to be the applicable criterion (2, p. 790). As the results indicate (Table 2), the yield load predicted by Equation 4 appears to agree better with the actual behavior of the beams than the load predicted by Equation 3. Neither criterion predicted the actual yield loads, perhaps because of the premature buckling described above.

Table 2. Beam properties and results for Bower's equations.

Beam	$\frac{H}{D}$	Hole	$\frac{a}{H}$	P_y, kips (Eq. 3)	P_y, kips (Eq. 4)	P_u, kips (Eqs. 5-8)
E	.67	End	.90	73.0	31.5	12.06
			1.20	73.0	39.8	18.72
		Ctr.	1.20	131.0	70.5	64.4
F	.80	End	.75	27.8	19.6	4.42
			1.00	32.6	28.0	6.24
		Ctr.	1.00	88.1	66.1	59.8

for both beams, $A_f/A_w = 0.533$
$F_v = 14.5$ ksi
$F_b = 22.0$ ksi
$V_p = 78.0$ kips
$M_p = 1484$ inch-kips

Observed yield loads
Beam E 12 kips ±
Beam F 4 kips ±

For comparison, the yield load of the solid beam, assuming no buckling occurred, would be 65 kips.

D. Prediction of Ultimate Load

A simple method of predicting the ultimate load of the beams would be to calculate the plastic moment of the tee sections and equate this to the bending moment expressed as a function of the applied load. For Beams "E" and "F" respectively, the plastic moments of the tees are 30.9 and 15.4 inch kips, and the corresponding ultimate loads are 13.7 and 6.8 kips. These values are slightly greater than the actual yield loads, but much lower than the failure loads of the beams, even with buckling as the mode of failure.

Bower has published a lower bound solution for the ultimate strength of beams with rectangular web holes which experimental results indicate to be conservative (2, p. 795; see also Figure 25). The solution leads to a system of four equations:

$$\left(\frac{V}{V_p}\right)^2 = k_2^2 - \left(2k_1\frac{A_f}{A_w}\right)^2 \tag{5}$$

$$(k_2)^2 = \left(\frac{2k_1A_f}{A_w}\right)^2\left[1+\frac{0.75\left(1-\frac{H}{D}-\frac{1}{2}k_2\right)^2}{\left(\frac{H}{D}\right)^2\left(\frac{a}{H}\right)^2}\right] \tag{6}$$

$$\frac{M}{M_p} = 1 - \left[\frac{\frac{4k_1A_f}{A_w} + \left(\frac{H}{D}+k_2\right)^2}{1+\frac{4A_f}{A_w}}\right] \tag{7}$$

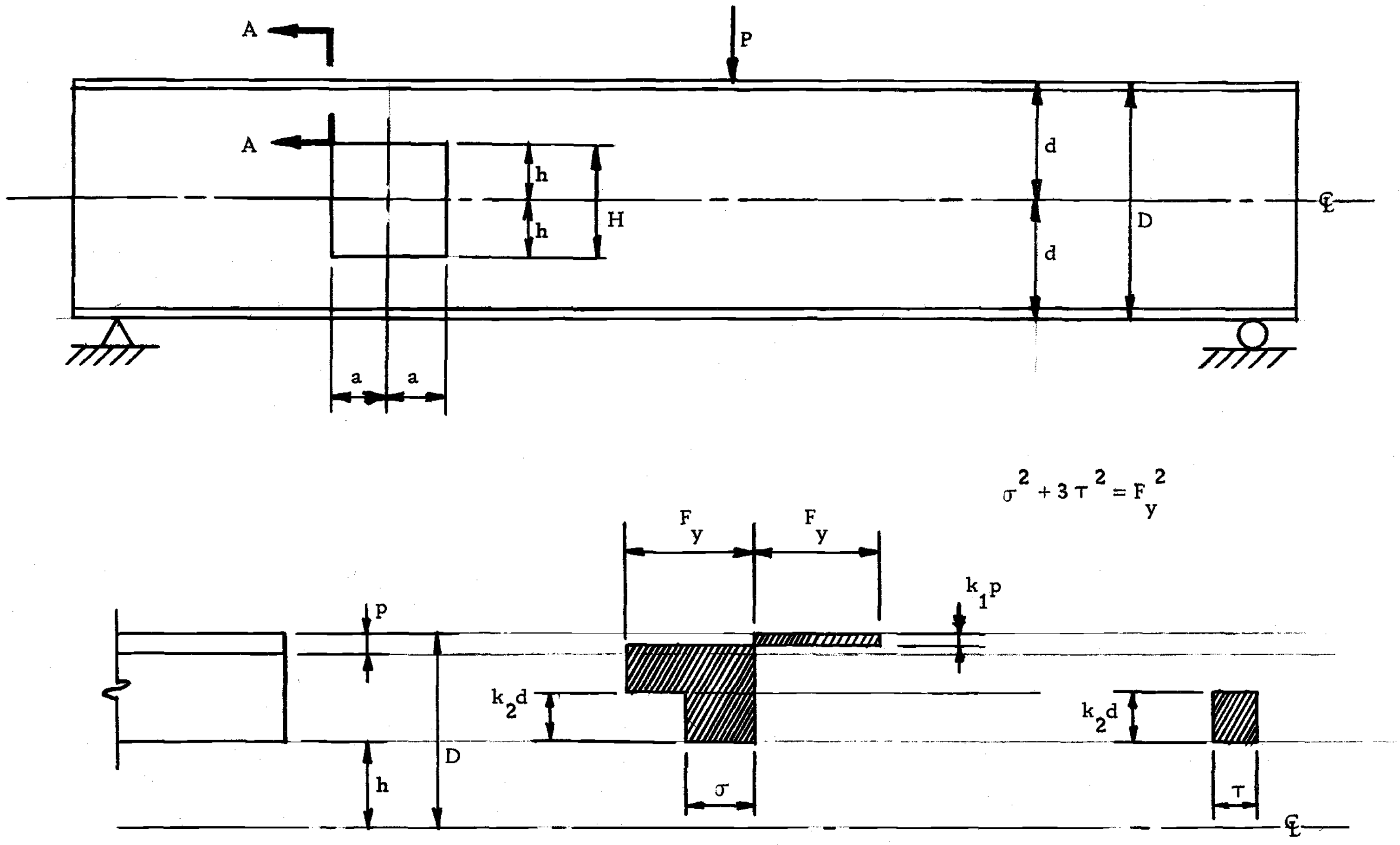

Stress distribution at Section A-A

Figure 25. Bower's lower bound solution for ultimate strength.

$$k_2 \leqq 1 - \frac{H}{D} \tag{8}$$

where V_p and M_p are the plastic shear and moment of the gross beam section and k_1 and k_2 are defined as indicated in Figure 25. The writer solved these equations by assuming values of k_2 between 0 and $1 - H/D$, substituting these into Equation 6 to find k_1, then substituting corresponding values of k_1 and k_2 into Equations 5 and 7 to find V/V_p and M/M_p. The result is an interaction diagram for a particular hole in a beam. For any given load, the shear and bending moment and thus V/V_p and M/M_p can be found; the shear and moment ratios for any other load will lie along a line through this point and the origin of the interaction diagram. The ultimate load can then be located as the intersection of the interaction diagram with the line describing the shear-moment relationship for the loading applied. For the beams tested by the writer, the ultimate load fell in the region of the interaction diagram controlled by the shear alone $(k_2 > 1 - H/D)$ for holes where $V \neq 0$, and for the center holes $V = 0$ and $k_2 = k_1 = 0$, which greatly simplified the solution of the equations for the ultimate load. The results are presented in Table 2. Surprisingly, the ultimate loads predicted for three of the holes agree well with the actual yielding of the gages For the first interior hole in Beam "F," some gages recorded yielding at lesser loads and some at greater loads.

Bower's solution did indeed conservatively predict the ultimate load of both beams, even though both failed by different forms of buckling. (See Figures 15 through 22, 26 and 27.)

For comparison, the ultimate load of the beams based on their reaching the plastic moment is 75.2 kips.

E. Deflections

For hand computation, a simple way to estimate the deflection of the beams is as the sum of the deflection of the corresponding solid beam plus the deflection of each tee section acting as a fixed-end beam under a shear loading. For the latter component, the deflection is

$$\Delta = \frac{VL^3}{12E(2I_t)} + \frac{1.2VL}{2A_tG} \qquad (9)$$

The results are presented in Table 3 and Figures 26 and 27. The errors varied from 4% to 28% of the measured deflections, the smaller errors being for Beam "F" where the deflections were larger. It is the writer's belief that part of the error is due to rotation of the web posts between holes, making the assumption of full fixity at the ends of the tees invalid. T.J. McClellan (10) has suggested that another error may be due to including the moment of inertia of the flange twice, once in each part of the deflection. It is also worth noting that the precision of measuring the deflections is ± .05" at best, and

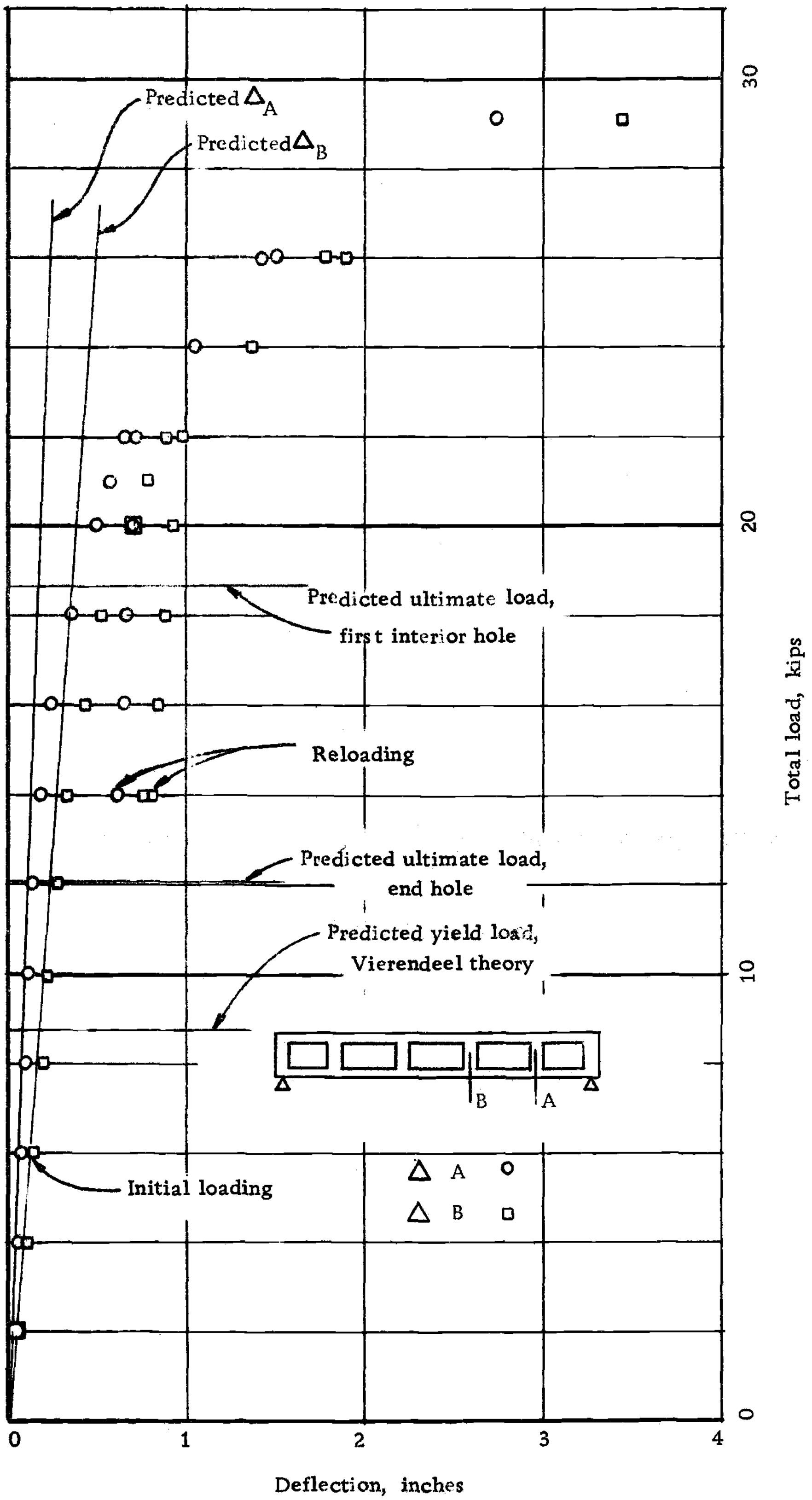

Figure 26. Beam "E." Load vs. deflection.

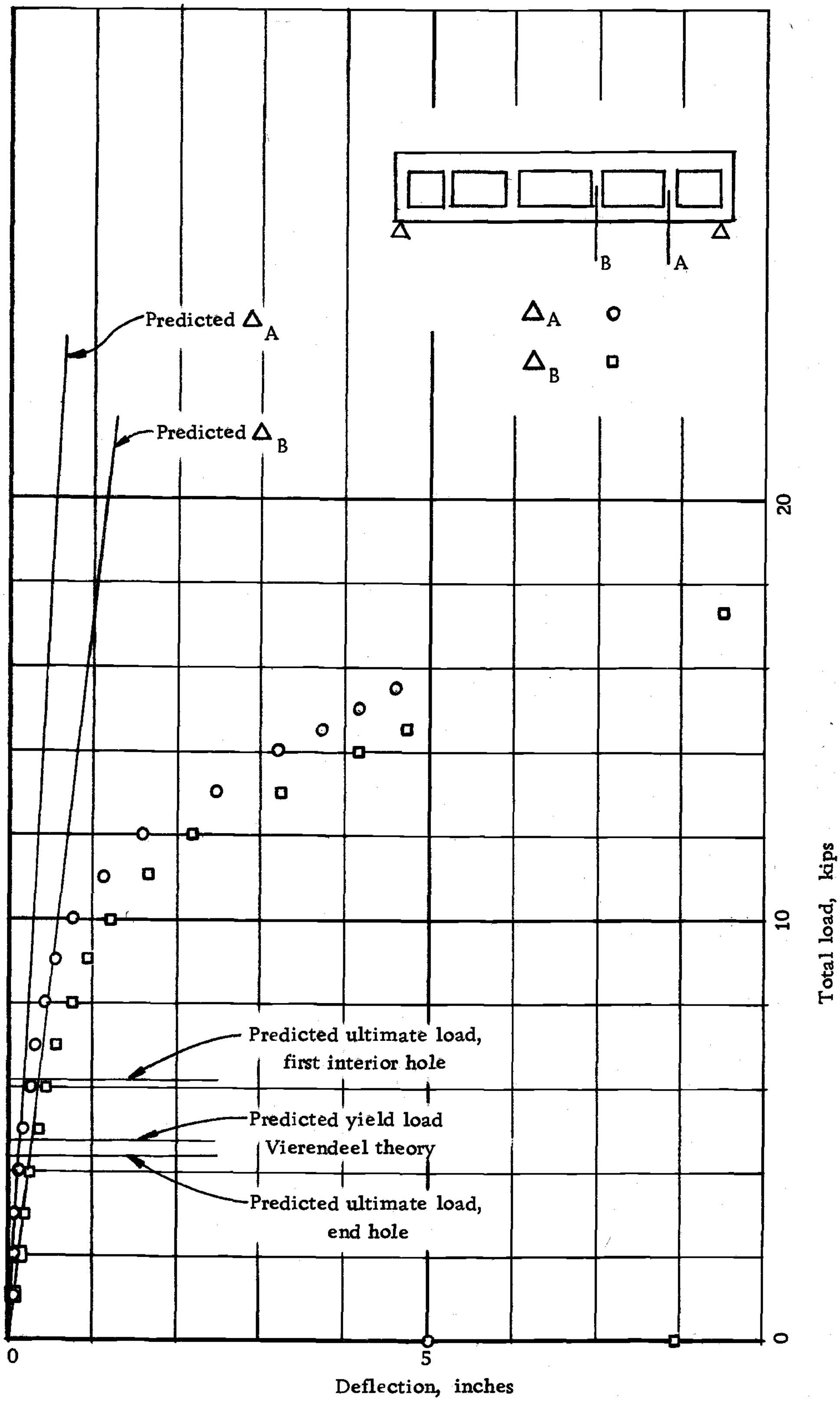

Figure 27. Beam "F." Load vs. deflection.

actually probably closer to ± .10''; the errors at yield load in each beam are no larger than this, and probably insignificant for design purposes.

Table 3. Calculated vs. measured deflections.

Beam	Hole	Deflection per Unit Load, inches per kip		
		Measured	Calculated	Error
E	End --- Ctr.	.0121 .0223	.0087 .0179	.0034 .0044
F	End --- Ctr.	.029 .058	.026 .056	003 .002

V. CONCLUSIONS

The Vierendeel theory appears to be valid for predicting elastic stresses for beams with ratios of hole depth to beam depth up to .80 and hole length to width up to 2.4, where $V \neq 0$. (Where $V = 0$, the "couple plus tee-bending theory" may be better, but in any case the effect of the holes will be much less severe than where a shear exists at the hole.) For analysis by hand, the precision involved in trying to locate the exact position of the inflection point in the tee sections does not appear to be warranted for design purposes. Although large stress concentrations are known to exist at the corners of the holes, they did not appear to affect the strength of the beams tested in this project. Bower himself has admitted that ". . . it would not be practicable in most cases of statically loaded beams, to design against yielding" (2, p. 791). It is not known whether Bower's yielding criteria are applicable to beams in this range, but his solution for the ultimate strength of such beams proved to be conservative. Deflections of the beams can be estimated with sufficient accuracy for design purposes as the sum of the deflections of the corresponding solid beams and the deflections of the tee sections as fixed-end beams under a shear loading. The tee sections do not appear to become unstable under large stresses, nor do the corners of the holes appear critical if cut to a small radius as those described herein were;

however, buckling of the web needs to be considered where holes are spaced closely together, and as with any beam, lateral bracing must be provided to prevent flange buckling.

The writer suggests that further research in this area be directed toward examination of Bower's yield strength and ultimate strength criteria, and especially toward testing of beams with holes eccentric to the centroidal axis, about which little is known even today.

BIBLIOGRAPHY

1. Baes, Louis. Rigid frames without diagonals (the Vierendeel truss). Transactions of the American Society of Civil Engineers 107:1215-1228. 1942.

2. Bower, John E. Design of beams with web openings. Journal of the Structural Division, American Society of Civil Engineers 94:783-807. March, 1968.

3. ________________ Elastic stresses around holes in the web of wide-flange beams. Journal of the Structural Division. American Society of Civil Engineers 92:85-101. April, 1966.

4. ________________ Experimental elastic stresses in wide-flange beams with web holes. Journal of the Structural Division, American Society of Civil Engineers 92:167-186. Oct., 1966.

5. ________________ Suggestions for research - holes in beam webs. Committee correspondence, Subcommittee 5 - Castellated beams, Monroeville, Pa. January 19, 1966.

6. ________________ Ultimate strength of beams with rectangular holes. Journal of the Structural Division, American Society of Civil Engineers 94:1315-1337. June, 1968.

7. Cato, Stuart Leslie. Web buckling failure of built-up girders with rectangular holes. Master's thesis. Corvallis, Oregon State University, 1964. 37 numb. leaves.

8. Hosain, M. U., and W. G. Speirs. Failure of Castelated (sic) beams due to rupture of welded joints. Acier-Stahl-Steel (Brussels) 36:34-40. Jan., 1971.

9. Landers, William. Web stresses in Vierendeel girders. Unpublished research. Corvallis, Oregon State University Engineering Experiment Station, 1965.

10. McClellan, Thomas J. Private communication. 1971.

11. Roark, Raymond J. Formulas for stress and strain. 4th ed. New York, McGraw-Hill, 1965. 432 p.

12. Russell, William Clyde. Experimental studies of Vierendeel beam analysis. Master's thesis. Corvallis, Oregon State University, 1966. 62 numb. leaves.

APPENDICES

NOTATION

A_f = bp = area of one flange

A_t = cross-sectional area of the tee section above or below a hole

A_w = Dt = gross web area

C = axial compression acting on a tee section according to the couple-plus-tee bending theory

D = beam depth

E = modulus of elasticity (29 million psi)

F_b = bending stress allowed by AISC Design Specification

F_v = shear stress allowed by AISC Design Specification

F_y = yield point of steel

G = shear modulus (assumed to be 0.4 x E)

H = depth of hole

I_b = moment of inertia of the beam taken at a hole

I_t = moment of inertia of the tee section

M = bending moment

M_p = plastic bending moment of the gross beam section

P = total load on the beam (see Figure 2a)

T = axial tension acting on a tee section according to the couple-plus-tee bending theory

V = shear force

V_p = plastic shear force of the gross beam section (taken as $(F_y/\sqrt{3}) \times A_w$)

a = half length of a hole

b = flange width

c_t = distance from centroid of tee to outside face of flange (see Figure 1a)

d = half depth of beam

f_a = axial stress in the beam

f_b = bending stress in the beam

f_{bg} = bending stress at a hole, computed using the gross beam section

f_t = total longitudinal stress (axial plus bending) in the beam

f_{vg} = shear stress at a hole, computed using the gross beam section

h = half depth of hole

k_1 = distance from outside face of flange to plastic neutral axis (see Figure 25)

k_2 = fraction of web depth yielded in combined bending and shear at a hole (see Figure 25)

p = flange thickness

t = web thickness

x = horizontal distance from point of inflection in tee section to point at which bending stress is computed.

y = vertical distance from centroid of net beam section to point at which bending stress is computed

y_t = vertical distance from centroid of tee section to point at which bending stress is computed

ϵ = strain

σ = bending stress in beam web

τ = shear stress in beam web

subscript u indicates plastic condition
subscript y indicates yield condition

BEAM "E" STRAINS (microinches per inch)

Load	Gages								
P	L-1	L-2	L-3	L-4	L-5	L-6	L-7	L-8	L-9
2	+ 18	- 45	- 72	- 279	+ 283	+ 72	- 10	- 10	- 14
4	24	76	145	558	564	145	20	24	29
6	24	100	219	831	842	219	27	36	44
8	22	123	291	1101	1114	292	38	46	57
10	16	149	362	1370	1380	373	49	55	70
12	13	172	443	1691	1642	462	56	68	88
14	9	190	601	2454	1930	601	43	103	188
16	+ 1	210	970	3970	5776	1752	- 7	162	341
18	- 9	226	2015	7612	8944	3539	+ 12	205	455
20	22	231	4148	12972	13906	5742	31	247	570
14	18	149	6022	17914	16558	8068	73	243	606
16	26	166	6100	18199	16833	8142	65	253	624
18	22	202	6166	18456	17085	8213	58	268	640
20	22	224	6239	18750	17374	8295	49	277	657
22	31	246	6344	19186	17793	8426	46	288	670
24	52	227	10048	29301		13091	55	330	768
26	- 44	- 211	-15958			+19877	+ 70	- 378	- 876

Load	Gages								
P	L-10	L-11	L-12	L-13	L-14	L-15	L-16	L-17	L-18
2	+ 9	+ 7	+ 13	- 104	+ 58	+ 281	- 262	- 56	+ 106
4	14	14	24	209	115	558	527	112	210
6	22	19	36	313	173	833	786	168	309
8	27	25	46	414	227	1105	1046	221	411
10	35	33	59	509	290	1374	1293	273	516
12	+ 32	38	74	619	366	1657	1554	345	621
14	- 28	+ 25	105	878	849	3199	2004	471	878
16	180	- 27	169	1416	2379	6559	2859	804	1186
18	287	61	216	2115	3935	10478	6928	1736	1908
20	394	92	262	3484	6638	16992	12611	3638	3031
14	468	123	251	4993	9407		17244	5932	4028
16	468	121	261	5103	9471		17513	5990	4125
18	470	119	268	5201	9529		17757	6045	4213
20	465	118	282	5309	9604		18044	6105	4310
22	455	115	289	5430	9710		18439	6194	4421
24	506	110	350	8375	14159		28000	9647	6870
26	- 580	- 133	+ 390	- 6873	+20873			-14577	

BEAM "E" STRAINS

Load	Gages								
P	L-19	L-20	L-21	L-22	L-23	L-24	L-25	L-26	L-27
2	+ 33	- 70	- 204	+ 210	+ 66	- 33	- 30	- 26	- 21
4	63	141	410	413	131	64	62	54	44
6	94	210	613	617	200	98	94	81	64
8	127	280	820	818	263	130	122	106	88
10	162	354	1021	1026	325	162	154	128	108
12	194	420	1226	1231	390	197	183	154	128
14	228	485	1432	1401	445	221	207	182	152
16	267	568	1685	1605	515	249	241	212	182
18	302	647	1929	1772	573	275	266	244	201
20	355	741	2275	1984	651	306	303	264	217
14	281	583	1869	1428	489	208	211	192	169
16	314	654	2087	1626	548	249	248	222	192
18	344	719	2275	1814	602	281	274	247	210
20	377	793	2485	2019	668	317	303	272	234
22	413	871	2722	2230	732	352	333	297	252
24	555	1292	3841	2551	860	350	367	306	232
26	+ 811	- 2077	- 5949	+ 3003	+ 988	- 410	- 443	- 326	- 195

Load	Gages								
P	L-28	L-29	L-30	L-31	L-32	L-33	L-34	L-35	L-36
2	+ 20	+ 29	+ 29	- 91	+ 21	+ 174	- 171	- 18	+ 100
4	41	53	58	187	40	340	342	38	194
6	59	77	88	277	58	510	509	58	283
8	77	98	115	358	82	678	679	77	375
10	97	120	147	447	102	841	843	92	361
12	116	143	179	537	111	1015	996	119	555
14	129	166	204	621	130	1167	1143	137	634
16	145	195	238	728	154	1352	1321	157	730
18	158	218	264	810	177	1510	1476	177	820
20	171	243	305	918	212	1696	1670	204	927
14	109	179	228	663	153	1220	1194	136	702
16	125	198	254	755	191	1380	1366	160	792
18	144	219	287	848	186	1534	1529	183	866
20	156	234	307	939	222	1693	1699	211	951
22	174	265	339	1032	246	1863	1875	232	1039
24	176	297	384	1254	265	2198	2167	236	1283
26	+ 79	+ 294	+ 481	- 1686	+ 417	+ 2878	- 3210	- 501	+ 1593

BEAM "E" STRAINS

Load	Gages								
P	L-37	L-38	L-39	L-40	L-41	L-42	L-43	L-44	L-45
2	- 40	- 32	- 17	+ 18	+ 28	+ 39	- 39	- 32	- 26
4	79	70	40	35	56	78	78	65	52
6	109	109	71	53	85	113	117	99	78
8	146	141	93	77	116	151	153	130	102
10	176	171	114	95	146	190	194	160	125
12	213	203	136	115	172	229	230	192	151
14	248	233	160	129	201	261	264	218	174
16	294	268	174	149	232	303	307	257	200
18	333	298	192	175	261	337	339	287	226
20	374	336	221	211	298	376	381	322	257
14	261	236	148	187	231	278	272	233	191
16	297	267	168	204	257	317	309	264	212
18	340	305	201	212	276	338	343	292	238
20	379	333	219	226	301	372	379	324	265
22	414	364	242	239	326	407	415	352	289
24	452	402	275	301	383	461	453	398	332
26	- 556	- 484	- 330	+ 319	+ 410	+ 493	- 546	- 446	- 373

Load	Gages								
P	L-46	L-47	L-48	L-49	L-50	L-51	L-52	L-53	L-54
2	+ 23	+ 30	+ 35	- 38	- 34	- 24	+ 26	+ 32	+ 34
4	47	62	73	73	58	51	51	62	68
6	68	92	109	110	99	75	76	93	103
8	92	122	147	145	133	98	99	125	140
10	115	154	176	183	164	123	114	166	177
12	139	186	212	215	197	150	136	196	214
14	163	215	245	254	228	173	157	224	247
16	177	244	289	286	264	205	181	255	284
18	202	273	323	316	296	239	186	280	317
20	228	308	365	352	331	273	190	312	362
14	172	237	279	253	240	201	124	229	279
16	196	270	312	291	274	226	150	261	309
18	200	283	334	322	303	251	153	272	332
20	221	311	369	355	335	278	172	301	364
22	243	339	406	389	367	306	192	330	397
24	269	389	474	466	433	340	198	368	464
26	+ 277	+ 422	+ 525	- 539	- 490	- 395	+ 187	+ 387	+ 515

BEAM "E" STRAINS

Load	Gages								
P	R-1-H	R-1-V	R-1-30°	R-1-150°	R-2-H	R-2-V	R-2-30°	R-2-150°	R-3-H
2	- 138	+ 18	- 105	- 200	+ 129	+ 24	+ 219	+ 97	- 87
4	277	24	208	400	257	41	427	195	173
6	412	24	303	604	388	49	631	290	257
8	544	22	403	812	520	56	835	386	339
10	677	26	507	1014	640	57	1038	485	423
12	823	22	617	1231	819	81	1416	637	503
14	982	20	744	1493	1118	263	2502	1042	592
16	1303	+ 22	999	2039	1396	422	1215	508	700
18	1785	- 5	1448	2934	1167	588	944	+ 366	782
20	2895	71	2556	5254	868	944	627	- 28	893
14	4140	103	1136	4784	114	1275	300	+ 249	662
16	4271	109	1178	4922	157	1271	322	274	746
18	4385	109	1214	5037	188	1278	343	300	835
20	4515	116	1257	5183	215	1281	343	306	921
22	4755	128	1308	5450	237	1325	343	296	1002
24	5289	- 346	- 830	5313	+ 201	1499	329	397	1073
26	- 1839	+ 116	+ 360	- 2135	+ 245	+ 1193	+ 166	+ 358	- 1118

Load	Gages								
P	R-3-V	R-3-120°	R-3-240°	R-4-H	R-4-V	R-4-30°	R-4-150°	R-5-H	R-5-V
2	+ 4	- 72	- 20	+ 83	+ 33	+ 148	+ 74	- 12	+ 13
4	- 10	169	48	164	63	295	149	18	+ 7
6	33	269	78	244	90	440	220	26	- 6
8	51	372	113	328	119	585	294	33	20
10	74	468	153	403	145	732	360	40	39
12	100	574	186	487	177	867	433	49	58
14	112	676	203	547	223	985	494	55	78
16	139	806	235	613	284	1132	564	58	104
18	168	925	252	679	341	1293	625	60	128
20	201	1112	277	755	405	1512	698	70	151
14	142	848	179	564	319	1585	489	48	105
16	169	962	210	642	350	1329	564	53	127
18	194	1075	236	700	375	1453	615	66	146
20	222	1176	282	780	413	1594	684	73	170
22	257	1312	308	860	449	1760	751	79	186
24	322	1494	355	1171	745	2674	849	88	226
26	- 413	- 1811	- 399	+ 1700	+ 1058	+ 4378	+ 1312	- 108	- 263

BEAM "E" STRAINS

Load	Gages					
P	R-5-30°	R-5-150°	R-6-H	R-6-V	R-6-30°	R-6-150°
2	- 20	+ 3	+ 1	+ 21	+ 9	+ 10
4	35	- 4	5	39	18	20
6	51	14	11	50	28	31
8	66	25	20	62	37	46
10	83	41	25	72	41	54
12	98	52	32	88	56	63
14	112	66	41	98	63	76
16	129	73	40	107	67	90
18	139	90	52	124	84	99
20	158	107	66	127	104	113
14	117	74	74	101	108	89
16	134	84	+ 71	114	110	101
18	146	104	66	115	110	99
20	162	122	65	133	120	104
22	172	134	69	144	123	115
24	193	160	94	158	165	140
26	- 221	- 198	+ 98	+ 201	+ 194	+ 139

BEAM "E" DEFLECTIONS (inches)

P	Δ_A	Δ_B
2	.02	.05
4	.05	.09
6	.07	.14
8	.10	.18
10	.12	.22
12	.14	.26
14	.18	.31
16	.24	.41
18	.34	.51
20	.49	.70
21	.55	.76
22	.65	.87
14	.58	.72
14	.61	.80
16	.64	.84
18	.65	.87
20	.68	.91
22	.70	.96
24	1.04	1.34
26	1.41	1.77
26	1.49	1.87
0	2.72	3.44

BEAM "F" STRAINS (microinches per inch)

Load	Gages								
P	L-1	L-2	L-3	L-4	L-4A	L-5	L-6	L-7	L-8
1	+ 123	- 190	- 341	+ 326		+ 183	- 121	- 5	- 4
2	240	365	662	632		354	236	11	7
3	362	551	992	948		532	352	17	- 12
4	501	751	1361	1522		810	497	73	+ 61
5	699	1104	1882	+ 2618		+ 1604	740	- 37	- 22
6	914	1568	2489	----		----	1018	+ 9	104
0	183	451	478	----		----	300	--	---
3				999		552			
3				984		543			
3				959		529			
4	669	1242	1876	1290		710	- 805	- 54	+ 17
5	794	1437	2215	1616		896	925	60	13
6	927	1671	2590	2019		1122	1053	67	+ 4
7	1224	2175	3275	3650		2226	1373	- 31	- 67
0	+ 354	- 659	- 806	+ 1417		+ 1005	520	--	--
6	1128	1900	2950	3478		2159	- 1262	- 47	+ 26
7	1274	2211	3380	3958		2435	1413	52	+ 16
8	1599	2847	4417	----		3044	1952	20	- 60
0	565	1319	1519	----		----	991	--	--
3				+ 1037	+ 1090	+ 566			
2	821	1708	2225	686	708	373	- 1236	- 6	- 5
4	1066	2099	2920	1361	1413	739	1477	24	16
6	1333	2557	3717	2125	2224	1165	1741	36	24
7	1484	2821	4158	2555	2701	1408	1875	41	26
8	1658	3179	4732	+ 3136	3360	1747	2040	45	34
9	2353	4577	7233	----	+ 6527	+ 4151	3345	- 10	101
10	+ 3769	7137	-11916	----	----	----	5981	+ 27	186
11	----	- 7687	----	----	----	----	11001	63	268
12	----	----	----				16117	95	326
13		----					-21191	+ 119	- 385

BEAM "F" STRAINS

Load	Gages								
P	L-9	L-10	L-11	L-12	L-13	L-14	L-15	L-15A	L-16
1	- 6	+ 8	+ 6	+ 3	- 129	+ 180	+ 258		- 308
2	11	14	11	6	253	349	495		597
3	- 18	19	15	9	378	525	728		894
4	+ 94	134	81	- 32	532	788	1113		1239
5	- 36	+ 24	+ 16	+ 16	830	---	----		1780
6	168	- 88	- 44	+ 69	1223	---	----		1506
0	---	--	--	--	446	---	----		640
3						516	953		
3						507	937		
3						494	915		
4	+ 28	+ 75	+ 49	- 16	- 992	+ 658	+ 1224		- 1912
5	23	78	50	11	1120	845	1590		2266
6	+ 9	+ 78	+ 47	- 8	1266	1057	1938		2576
7	- 105	- 20	- 5	+ 40	1703	2006	----		3359
0	---	--	--	--	768	658	----		1110
3							953		
6	+ 32	+ 8	+ 78	+ 10	1577	1734	1980		3056
7	+ 17	+ 107	78	15	1738	1995	2442		3472
8	- 99	- 3	14	+ 71	2355	----	----		4510
0	--	---	--	--	- 1296	----	----		- 1836
3						561	1054	+ 1031	
2	- 17	+ 14	+ 13	+ 9	- 1559	+ 371	+ 689	+ 675	- 2469
4	30	22	19	15	1821	730	1376	1348	2500
6	45	31	30	23	2106	1160	2167	2128	3804
7	47	38	32	30	2253	1410	2619	2582	4191
8	57	+ 38	+ 38	38	2430	1771	+ 3241	+ 3196	4691
9	163	- 57	- 18	94	3360	+ 4069	----	----	6895
10	296	184	92	151	5456	----	----	----	-10569
11	423	297	159	200	9286	----			-----
12	519	376	200	227	14623				-----
13	- 598	- 443	- 241	+ 259	-20901				

BEAM "F" STRAINS

Load	Gages								
P	L-17	L-18	L-19	L-20	L-21	L-22	L-23	L-24	L-25
1	- 165	+ 128	+ 71	- 151	- 244	+ 233	+ 125	- 72	- 15
2	318	253	135	290	474	444	238	140	29
3	479	376	203	431	704	656	353	205	41
4	663	529	243	588	962	962	532	224	77
5	975	828	338	795	1291	+ 1730	998	351	69
6	1391	1097	+ 453	1022	1646	----	1445	485	63
0	376	340	---	143	216	----	723	---	--
3						839	374		
3						866	371		
3						849	363		
4	1071	838	251	758	1202	1426	+ 474	- 251	- 72
5	1264	982	328	920	1470	2287	612	327	85
6	1438	1099	392	1050	1678	3353	728	392	96
7	1727	1490	+ 503	1319	2029	----	1156	- 533	- 86
0	676	567	---	279	353	----	306	---	--
3									
6	- 1735	+ 1356	+ 432	- 1189	- 1821	----	1054	432	88
7	1972	1514	504	1355	2074	----	1213	518	99
8	2578	1951	651	1683	2454		1797	668	85
0	1122	860	---	475	507	----	59		
3			224			708			
2	1462	1125	147	791	1019	476	302	148	27
4	1803	1379	283	1084	1498	927	526	291	54
6	2192	1659	427	1392	1991	1398	765	437	82
7	2402	1804	501	1549	2238	1646	892	508	96
8	2689	1974	578	1723	2487	1939	1037	583	106
9	3900	2642	698	2057	2854	2838	1475	727	92
10	- 6398	+ 4316	907	2494	4350	4263	2313	1019	65
11	----	----	1143	3034	3974	5159	3181	1322	47
12	----	----	1611	4354	5569	6294	4192	1722	27
13			+ 2225	- 5716	- 7833	+ 7584	+ 5465	- 2287	- 3

BEAM "F" STRAINS

Load	Gages								
P	L-26	L-27	L-28	L-29	L-30	L-31	L-32	L-33	L-34
1	- 18	- 20	+ 9	+ 13	+ 20	- 104	+ 126	+ 221	- 202
2	34	38	19	25	32	199	243	424	389
3	52	56	29	35	47	302	358	630	581
4	33	14	106	82	43	415	534	903	790
5	89	94	+ 48	57	78	583	981	1571	1041
6	149	179	- 10	24	126	765	1463	2237	1334
0	---	---	--			156	737	988	166
3									
3									
3									
4	54	- 52	+ 69	62	44	584	1213	1817	970
5	74	73	82	67	60	698	1357	2064	1193
6	91	80	86	84	73	793	1478	2268	1369
7	156	- 178	+ 35	62	112	1040	1522		1726
0	---	---	--			335			333
3							365	658	
6	113	123	65	74	95	962	741	1328	1560
7	138	151	65	87	114	1085	922	1643	1797
8	207	251	14	61	160	1396	1627	2705	2210
0						546	637		578
3								704	
2	35	41	24	0	46	767	887	452	1000
4	75	80	42	45	73	973	1121	896	1399
6	114	126	65	47	107	1181	1382	1359	1810
7	133	146	76	69	124	1292	1508	1584	2007
8	151	167	77	84	146	1414	1664	1881	2243
9	215	258	+ 44	57	199	1698	2294	2867	2712
10	301	382	- 25	+ 27	245	2113	3232	4377	3302
11	379	491	96	- 3	281	2731	4325	6110	3991
12	462	608	173	41	367	3688	5827	8529	4990
13	540	- 717	- 237	- 77	+ 432	- 5052	+ 6633	+ 3470	- 7147

BEAM "F" STRAINS

Load	Gages								
P	L-35	L-36	L-37	L-38	L-39	L-40	L-41	L-42	L-43
1	- 100	+ 100	- 18	- 13	- 11	+ 11	+ 13	+ 22	- 22
2	196	190	46	22	16	15	23	43	42
3	293	281	69	36	24	17	31	64	62
4	394	373	84	39	29	25	44	89	77
5	526	490	106	55	46	37	55	109	102
6	676	587	123	75	62	46	69	130	120
0	95								
3									
3									
3									
4	504	366	92	46	35	22	41	84	86
5	616	474	117	65	50	36	55	104	109
6	707	554	132	79	65	41	62	122	128
7	887	687	154	95	77	44	71	150	150
0	195								
3									
6	806	590	137	78	58	48	70	133	114
7	928	692	161	84	67	53	80	161	137
8	1149	951	178	97	69	56	89	193	154
0	335	164							
3									
2	543	354	45	35	30	23	20	44	44
4	736	359	86	58	48	43	44	82	86
6	948	756	132	86	68	55	69	128	124
7	1055	851	161	96	74	56	78	151	146
8	1174	953	184	110	87	59	86	174	163
9	1428	1153	204	141	119	87	116	204	187
10	1752	1466	224	163	143	96	130	229	206
11	2154	1799	235	189	180	126	151	241	224
12	2705	2149	255	205	195	120	165	270	245
13	- 3861	+ 2858	- 267	- 220	- 207	+ 126	+ 183	+ 293	- 256

BEAM "F" STRAINS

Load	Gages								
P	L-44	L-45	L-46	L-47	L-48	L-49	L-50	L-51	L-52
1	- 18	- 15	+ 18	+ 19	+ 21	- 18	- 20	- 23	+ 25
2	34	33	32	34	38	33	43	51	53
3	52	48	44	46	52	47	67	80	78
4	70	64	58	65	76	64	92	103	108
5	90	84	75	86	99	86	112	131	125
6	102	100	85	99	115	102	127	146	140
0									
3									
3									
3									
4	74	66	58	64	77	68	94	110	109
5	93	84	77	86	99	88	115	136	127
6	109	98	81	92	106	105	132	152	145
7	126	116	100	106	121	120	158	182	171
0									
3									
6	97	85	97	97	113	91	123	146	154
7	112	104	113	116	135	107	149	176	187
8	132	119	133	136	158	121	170	206	222
0									
3									
2	38	34	29	33	39	40	41	49	47
4	72	66	62	68	81	73	82	96	95
6	106	101	93	97	120	107	127	151	145
7	123	115	108	114	133	122	150	180	172
8	141	130	122	127	147	134	173	204	193
9	163	151	149	152	176	161	186	216	209
10	181	171	166	173	205	181	205	234	229
11	198	186	177	191	225	204	212	237	224
12	216	204	192	202	247	224	238	266	244
13	- 233	- 222	+ 210	+ 230	+ 264	- 243	- 243	- 258	+ 244

BEAM "F" STRAINS

Load	Gages								
P	L-53	L-54	R-1-H	R-1-V	R-1-315°	R-2-H	R-2-V	R-2-45°	R-3-H
1	+ 23	+ 19	- 139	+ 3	- 74	+ 131	+ 15	+ 75	- 97
2	44	35	270	- 1	149	255	14	135	186
3	62	43	405	0	224	381	16	203	282
4	87	58	553	+ 3	307	524	35	312	382
5	107	82	754	9	442	684	151	552	515
6	119	95	949	17	607	+ 531	276	816	653
0			132	+ 13	132	- 112	261	397	87
3						+ 432	61	298	
3						426	66	293	
3						413	66	285	
4	91	57	708	- 17	476	514	56	367	493
5	108	75	859	14	565	603	67	469	596
6	120	88	987	10	643	700	85	573	684
7	143	102	1185	19	915	+ 684	+ 236	+ 885	816
0			229	- 17	- 330				162
3						342	73	240	
6	131	96	1062	31	837	668	84	447	747
7	155	114	1210	31	951	776	100	551	853
8	181	133	1504	134	1399		250	921	959
0			414	- 151	- 725				191
3						+ 426	+ 70	+ 304	
2	41	35	700	159	899	282	64	208	394
4	82	69	978	164	1061	549	85	396	583
6	125	98	1262	159	1240	828	111	600	774
7	146	112	1411	158	1340	980	124	717	861
8	162	121	1567	169	1484	1140	156	876	963
9	183	156	2341	285	2373	1538	335	1421	1094
10	200	180	3575	518	3714	640	539	1482	1236
11	205	212	5358	914	5611	403	756	1089	1318
12	226	231	7032	1232	7946	366	774	541	1621
13	+ 239	+ 252	- 6733	- 1249	- 8151	+ 259	+ 712	+ 328	- 2108

BEAM "F" STRAINS

Load	Gages								
P	R-3-V	R-3-315°	R-4-H	R-4-V	R-4-45°	R-5-H	R-5-V	R-5-45°	R-6-H
1	- 14	- 57	+ 91	+ 10	+ 44	- 3	- 15	- 10	+ 8
2	31	111	173	+ 13	84	10	28	18	12
3	48	169	252	+ 12	120	13	44	26	12
4	59	227	332	- 31	92	18	59	34	22
5	64	297	421	+ 13	208	23	74	45	27
6	- 69	371	525	+ 71	342	36	77	54	31
0	+ 15	43							
3									
3									
3									
4	- 69	298	329	- 15	124	14	73	50	14
5	83	356	423	- 13	165	31	83	58	21
6	89	407	499	- 9	211	37	88	65	25
7	92	490	604	+ 57	348	48	99	77	21
0	7	102							
3									
6	94	449	531	+ 41	278	22	76	57	27
7	95	510	628	44	354	26	82	63	34
8	101	601	754	129	518	35	85	68	37
0	6	148		88	102				
3									
2	46	281	140	100	207	14	41	37	8
4	70	392	274	106	295	25	70	59	24
6	80	496	410	121	382	36	82	70	33
7	93	550	469	122	430	41	89	75	32
8	101	617	515	129	483	46	100	82	33
9	114	736	570	205	633	64	105	96	45
10	131	883	638	299	811	76	105	104	51
11	194	1125	713	390	1032	99	104	113	59
12	263	1471	802	481	995	101	82	99	61
13	- 317	- 1937	+ 432	+ 551	+ 730	- 122	- 9	- 51	+ 70

BEAM "F" STRAINS — BEAM "F" DEFLECTIONS (inches)

Load	Gages			
P	R-6- V	R-6-45°	Δ_A	Δ_B
1	+ 9	+ 6	.03	.06
2	12	6	.06	.12
3	12	5	.09	.17
4	11	5	.11	.23
5	18	7	.16	.33
6	22	8	.23	.44
0			.06	.09
3			.15	.27
3			.15	.27
3			.14	.27
4	9	6	.17	.33
5	10	7	.21	.40
6	10	7	.23	.45
7	10	3	.31	.57
0			.10	.16
3			.19	.35
6	16	13	.28	.51
7	23	14	.33	.56
8	33	19	.42	.73
0			.17	.24
3				
2	9	2	.23	.36
4	8	7	.29	.48
6	15	16	.36	.60
7	23	14	.38	.66
8	15	8	.42	.73
9	10	10	.54	.91
10	15	10	.76	1.20
11	+ 10	+ 12	1.12	1.65
12	- 4	- 5	1.59	2.18
12			1.70	2.33
13	- 45	- 39	2.43	3.21
14			3.20	4.18
14.5			3.68	4.71
15			4.14	
15.5			4.56	
17.3				8.5
0			5	7.9